ARMY RESEARCH LABORATORY

ARL

Modeling Workload for Target Detection From a Moving Vehicle With a Head-Mounted Display and Sound Localization

Christopher C. Smyth

ARL-TR-2759   JUNE 2002

Approved for public release; distribution is unlimited.

20020805 161

NOTICES

Disclaimers

Army Research Laboratory
Aberdeen Proving Ground, MD 21005-5425

ARL-TR-2759   June 2002

Modeling Workload for Target Detection From a Moving Vehicle With a Head-Mounted Display and Sound Localization

Christopher C. Smyth
Human Research & Engineering Directorate

Approved for public release; distribution is unlimited.

Abstract

The effect of indirect vision systems on target detection and recognition is of interest to designers of future combat vehicles. In this report, a model of target detection and mental workload is described for an indirect vision system with a micro-state task time line analysis of attention workload. The model is based on the results of a field study in which participants detected and identified pop-up targets on an outdoor range from a stationary and a moving vehicle while using a head-mounted display (HMD), with and without sound localization and with direct viewing as a control. A head-slaved camera mounted on top of the vehicle provided the image to the HMD. As a result of the study, a target detection and identification model is derived for the different treatments from the data via regression analysis. The effect of indirect vision on mental workload is determined from the subjective ratings of perceived task loading that were reported in the field study. Along with the perceived workload, the study participants rated the mental measures of task-allocated attention, situational awareness, and motion sickness. Because of collinearity, the perceived workload is regressed on the factorial components of a cognitive loading space derived from a factorial analysis of the mental measures. Following rotation to a "skills-rules-knowledge" cognitive processing space derived from the clustering of the measures, the perceived workload is shown to be a function of the skill- and rule-based components. On this basis, a micro-state time line model is proposed for the task information processing. In addition to the attention allocated to the targeting task, the model includes attention to cognitive maps for target orienting by the audio cues and the monitoring of the internal somatic state for motion sickness. Further, the model includes switching between tasks (detection to identification) and the initial orienting and subsequent suppression responses to audio cues and body movements as intrusive stimuli. The task-loading measures generated by the model are compared to the reported values with significant results. Finally, the model results are used to construct information flow networks for task analysis workload simulation studies. The model is intended for future work in predicting fatigue and performance errors that are induced by mental workload during indirect vision targeting.

ACKNOWLEDGMENTS

INTENTIONALLY LEFT BLANK

Contents

INTENTIONALLY LEFT BLANK

MODELING WORKLOAD FOR TARGET DETECTION FROM A MOVING VEHICLE WITH A HEAD-MOUNTED DISPLAY AND SOUND LOCALIZATION

---

1. Introduction

In this section of the report, we describe the background rationale for the research and discuss factors to be considered in the modeling effort. We comment on the effects of camera and display selection on performance as well as the benefits of sound localization for target detection. We suggest criteria for optimal crew performance, including workload and situational awareness (SA), and we discuss the potential effects of motion sickness. Finally, we comment on the field study and experimental data used in the modeling.

1.1 Background

The Army needs combat vehicles that are smaller, lighter, more lethal, survivable, and more mobile to support a rapidly deployable force. Combined with the need to assimilate and distribute more information to, from, and within the vehicle as the Army moves toward a digital battlefield, there is the need for an increase in vehicular and command, control, communications, computers, and intelligence systems integration and performance. Consequently, the Army will need sophisticated, highly integrated crew stations for these future combat vehicles. In support of this effort, the Tank-Automotive Research, Development, and Engineering Center (TARDEC) is developing the TARDEC crew integration and automation test bed (CAT) advanced technology demonstrator (ATD). The purpose of the CAT ATD is to demonstrate crew interfaces, automation, and integration technologies required to operate and support future combat vehicles. The results can dramatically increase the operational effectiveness and capabilities with fewer crew members, thereby contributing to smaller and lighter weapons systems.

1.2 Indirect Vision Systems

To satisfy the Army requirements for reduced gross weight and lower silhouette, as well as the need for increased crew protection against ballistic and directed energy threats, designers of future armored combat vehicles will place the crew stations deep within the hull of the vehicle. For protection against direct and indirect fire as well as chemical and biological agents, the crews will operate with their hatches closed and sealed. High intensity combat lasers that can penetrate direct vision blocks may force the crew to operate on the battlefield in a "buttoned up" mode, with indirect vision systems for driving and target search and engagement. The conventional optics, which consist of periscopic vision blocks and optical sights, will be replaced by electronic displays at each crew station and by externally mounted camera arrays on the vehicle. These vision systems will show computerized digital images that are electronically acquired by the camera arrays. The crew member will see a selected portion of the computerized display buffer

that depends on his role and viewing direction. No doubt, by the incorporation of virtual reality display and camera components, future vision systems will appear to have a "see-through armor" capability with a seemingly direct view of the external scene through the armored hull of the vehicle.

1.3   Camera Selection

Before indirect vision systems can be considered for future vehicle designs, combat and materiel developers will need to know the potential impact upon the crew's combat performance. During night operations, replacing the vision blocks with infrared thermal viewers improves the crew performance by enhancing visibility at low light levels. In daylight conditions, however, the use of indirect vision may cause a reduction in visual performance and SA. This is because of the decrease in visual resolution and field of view (FOV) of the current sensors and displays as compared to vision of the human eye through vision blocks. This reduction in visual performance may reduce overall combat performance. Further, the choice of camera configuration and placement on the vehicle can influence performance. For example, a single telescopic camera used in target search and detection may not have the performance of a multiple array of such cameras placed about the vehicle and electronically integrated to give a more naturally panoramic view.

1.4   Visual Display Selection

The visual display selection will influence the vehicle design. The design may use a set of panel-mounted displays, either cathode ray tube (CRT) or flat panel liquid crystal displays (LCD), which are fixed in a panoramic arrangement about the crew member's station. Another option is the use of a miniature head-mounted display (HMD) attached to the crew member's helmet. The display scene of the HMD can be slaved to head movements with a head tracker and for that reason, may appear more natural but with a limited FOV. Compared to the CRT and LCD panel displays, the use of the HMD significantly reduces the size, weight, and power requirements for the crew station. However, the miniature displays that are currently available cannot match the brightness and resolution of the larger panel systems and may result in degraded crew performance. The display selection will also have an impact on the crew size needed to operate the armored vehicles of the future. We can expect in the future to have two- or three-person crews available. The form of computerized aiding used with the crew member's electronic associate for the armored crew station is influenced by the display design. A panoramic design of panel displays for a two-person crew seated together may facilitate team interaction and performance. In contrast, the use of HMDs may tend to isolate the crew members while requiring increased electronic communication between them.

1.5   Sound Localization

One problem of interest is the effectiveness of an HMD in target detection and identification with a head-controlled telescopic sight. A problem for target detection and identification with

indirect vision systems is the inherently low visual acuity and limited FOV provided by the current display technology. On the modern digital battlefield, the crew may have advanced knowledge of the target's location. In this case, auditory directional cueing by sound localization should facilitate visual target detection by orienting the gunner toward the target. The choice of auditory cueing for a visual task reduces cognitive interference. This is shown by the literature about interference for performance of concurrent tasks with directed attention, time sharing, and workload (Wickens, 1992). Cueing can act as a secondary task supporting or interfering with the primary task, depending on the display format design. Wickens (1992) reports poor time sharing for two visual displays so spatially separated that both cannot be accessed by foveal vision simultaneously. However, displays of different modalities such as visual and auditory can have reduced interference with task performance.

1.6 Optimal Crew Performance

Another factor in the display design is the need to maintain SA and a mental model of the task. As noted by Endsley (1993b), SA is a precursor to optimal performance since a loss in awareness impacts decision making and leads to a risk of performance error. However, human operators can perform well with less-than-optimal display systems by increasing their efforts to meet the more demanding workload. The resulting increase in flow of information and tasks may result in a loss of SA; this is because the ability of humans to process information is innately limited. For this reason, besides demonstrating improved performance, a further criterion is that the display system should not generate excessive workload nor decrease SA.

1.7 Motion Sickness

Another factor influencing crew performance is the possibility of motion sickness, which can occur in an enclosed cab area with spatial disorientation. As noted by Yardley (1992), motion sickness is provoked by sensory conflict between the visual and sensorimotor activities that involve the vestibular system through head movements. Associated is a constellation of mainly autonomic symptoms such as pallor, drowsiness, salivation, sweating, nausea, and finally, vomiting in the more severe cases of motion sickness. Although some individuals may eventually adapt to situations that initially provoke sickness (Yardley, 1992; Baltzley, Kennedy, Berbaum, Lilienthal, & Gower, 1989), others do not, and the occurrences may be severe enough to arrest task performance until the symptoms subside.

1.8 Experimental Field Study

Before indirect vision systems can be designed for future military vehicles, materiel developers will need to know the potential impact of design parameters on combat performance. In support of this effort, The Human Research and Engineering Directorate of the U.S. Army Research Laboratory (ARL) is providing human factors expertise in determining the effect of these new crew station technologies with a continuing series of studies and investigations. Because of this need, TARDEC asked ARL to investigate the effects of indirect vision upon target search and

detection. In this study, ARL conducted an experiment to determine the target detection and identification performance of vehicle crews using computerized indirect vision with HMDs and optical systems. Further, we investigated the effects of indirect vision on the mental workload measures of attention allocation and perceived workload, SA, and induced motion sickness. The results were compared to direct vision search as representative of a "see-through armor" vision system. The experimental methodology and statistical results are reported in a separate report (Smyth, 2002b). This report describes the modeling development for task performance and mental workload that was derived from the results of the field experiment. The next section summarizes the method and results of the study as background to the modeling effort.

2. Objective

A model of target search and mental workload is derived for an indirect vision system. As a result of the field study, a task performance model is derived for target detection and identification as a function of the experimental treatments. The effect of indirect vision on perceived mental workload is modeled with subjective measures of task-allocated attention, SA, and motion sickness that resulted from the field study. Following clustering relations among the measures, the perceived workload is regressed onto a skill-rule-knowledge (SRK) cognitive attention space derived for information processing. A micro-state activity model is proposed for the targeting task, and the perceived workload and task attention measures are related to the time line activities of the model processors. The model results are used in task analysis workload simulation of indirect vision target detection and identification.

3. Field Experiment

Described in this section as background information are the methodology used in the field study, task analyses of the detection and identification tasks, mental model and production rules used in the tasks, and a summary of the statistical results.

3.1 Methodology

In a field study, eight male participants detected and identified "pop-up" targets on an outdoor range from a stationary and a moving vehicle while using an HMD, with and without sound localization and with direct viewing as a control (Smyth, 2002b). The study was a repeated measures experiment with all participants experiencing all conditions in a counterbalanced manner. A head-slaved telescopic camera mounted on top of the vehicle provided the image to the HMD. With sound localization, the audio tones (intermittent at 0.5-second intervals), which

4

were controlled by an on-board computer, appeared to originate from the location of the target. The targets were raised for display and lowered one at a time via computer control by the personnel supporting the experiment. For each trial run, the experimenter raised a paddle to alert facility control to start the trial and then again following target detection and target identification. The support personnel recorded the detection and identification times by activating a computer key. Following detection, the participant used binoculars or zoomed the telescopic camera to identify the orientation of a Landolt ring on the face of the target board. Following identification, the target was lowered in preparation for the next trial. At the end of each counterbalancing block of trial runs, the participant rated questionnaires on measures of mental workload, including perceived workload, task attention, SA, and motion sickness.

3.2 Task Analysis

Figures 1 and 2 are flow diagrams of the task analyses for the target detection and identification in terms of the observable body movements and responses from the start of the trial run to the vocal response to the experimenter.
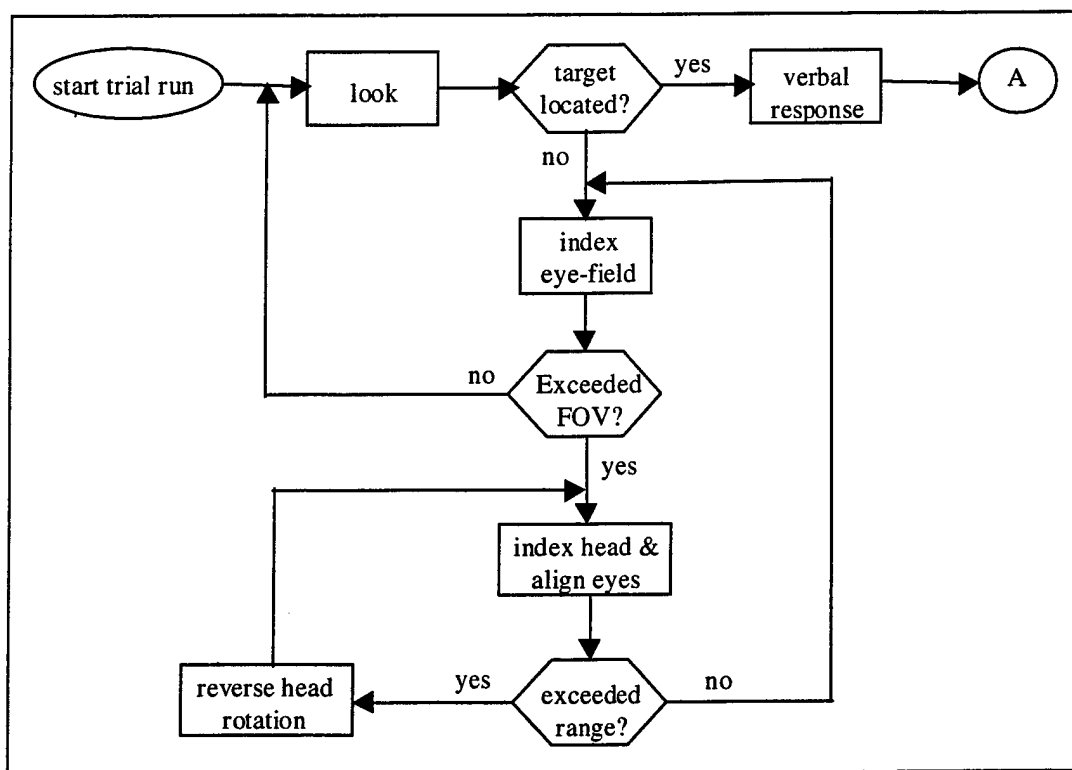
Figure 1. Task Analysis for Target Detection.
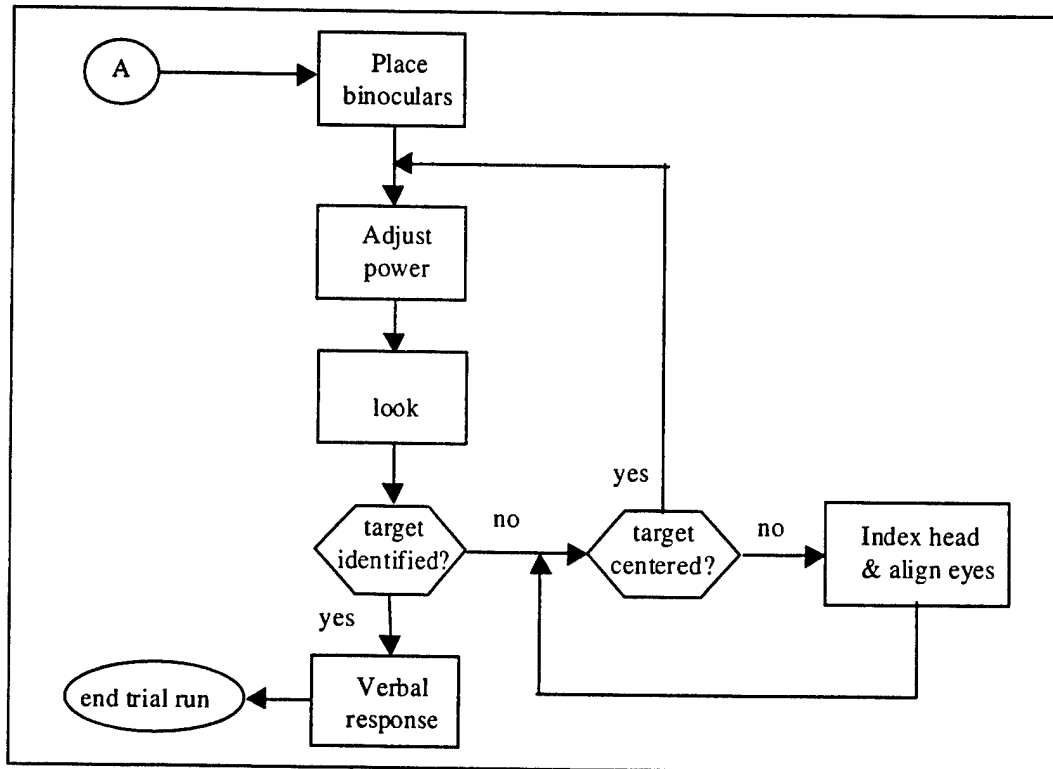
Figure 2. Task Analysis for Target Identification.

3.2.1 Detection

As seen from Figure 1, at the start of the trial run, the participant looks for the target with a visual glimpse and tells the experimenter if one is detected. In this process, he automatically segments the glimpsed image into target-sized shapes and compares them to a mental template that he has memorized. If no target is located, the participant continually indexes his eyes along the experimental facility for more visual glimpses. While doing this, he compares the scene to a mental model that he has of the terrain and perhaps to the locations of targets that he expects to find on the facility. When the participant's foveal vision is obscured by the side of the viewing device, he rotates his head sideways and realigns his eyes to repeat the viewing process. If he visually transverses the entire front of the target range without target detection, he will reverse his head motion to track back over the facility. Again, the participant has to maintain a mental map of the terrain and his location on the facility.

3.2.2 Identification

Following detection, the participant places the binoculars to his eyes and adjusts the magnification power while looking at the target. He or she continues to index his head orientation to keep the target centered while he adjusts the magnification. Similar comments apply to viewing with the HMD. In this process, the participant maintains a mental image of the target location in the surrounding scene to guide his vision during the adjustments. Furthermore,

he has an expectancy about the size and location of the Landolt ring on the target board, as well as the possible gap orientations. Upon identification, he tells the experimenter the gap orientation to complete the trial run.

3.2.3 Intrusive Tasks

Although the detection and identification tasks are serial in nature, Figure 3 contains flow diagrams for two tasks that are intrusive to the process: the responses to the sound cue and scene movement. A sound cue during detection will cause the participant to align his viewing direction with that of the apparent source. However, sound cueing will not aid identification once he has sighted the target, and he may decide to ignore the cue. In this case, the sound cue may impose an increased mental load because of the need to evaluate the intrusion. A change in the scene induced by vehicular motion should cause the participant to realign his viewing direction. In this case, he is revising and maintaining a mental model of the terrain and his location and orientation relative to the facility.

(a). Sound cue subtask.

(b). Body movement subtask.
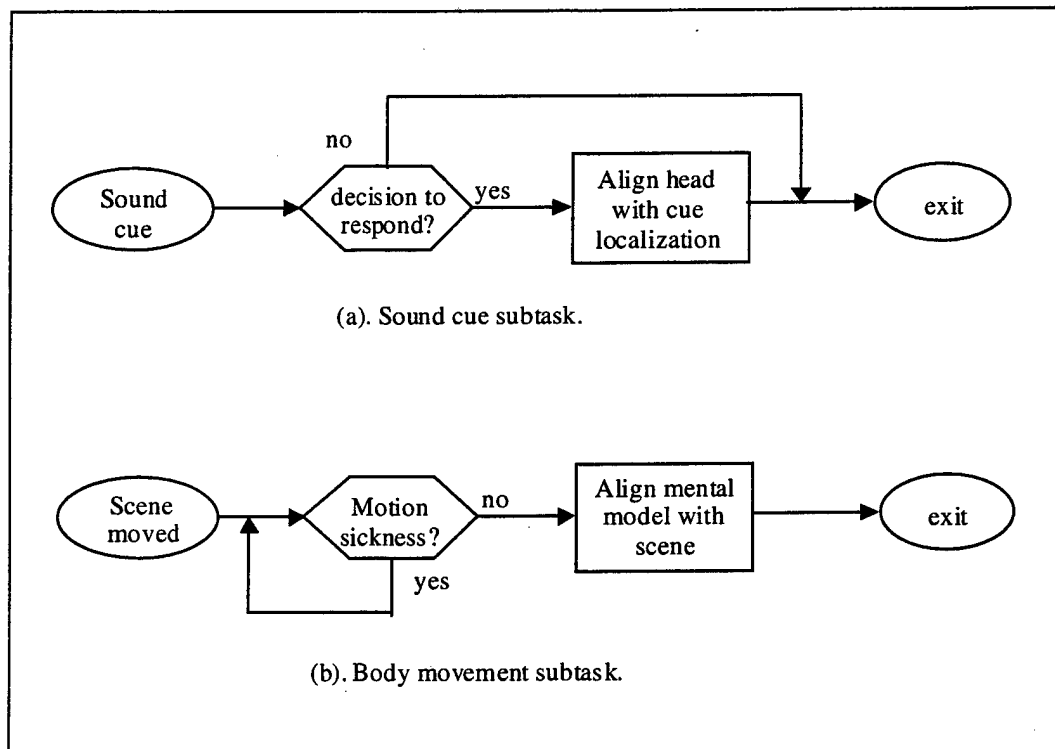
Figure 3. Intrusive Sub-tasks of Sound Cues and Body Movement.

3.2.4 Function and Task Allocation

Table 1 lists the allocation of functions and tasks for the target detection and identification. The table lists the human information processors and modalities, the operator interfaces, and the mental model maintenance that is involved by sub-task. The human processors include the perceptual with visual and acoustic modalities; cognitive with skill-based, rule-based, and

7

Table 1. Allocation of Functions and Tasks

Function / Task	Perceptual		Human Operator Cognition			Motor			Human operator interface				Mental Model Maintenance	
	visual	acoustic	skill	rule	know	ocular	voice	manual	Eliciting Event	Interface Display	Feed-Back	Follow-up Action	Task	Situation
target detection-														
orient view		x	x	x	x	x		x	start cmd	direct/HMD	rotate head	look	x	
look (glimpse)	x		x	x	x	x			oriented	direct/HMD	evaluate	decision	x	
target located	x		x	x	x		x		match	direct/HMD	verbal	identify	x	
index eye field	x		x	x	x	x			not located	direct/HMD	check scene	look	x	
shift view	x		x	x	x			x	exceeded FOV	direct/HMD	rotate head	align eye	x	x
align eyes	x		x	x		x			rotated head	direct/HMD	check scene	look	x	
reverse rotation	x		x	x	x	x		x	view off range	direct/HMD	rotate head	align eyes	x	x
target identification-														
place binoculars	x		x	x	x	x		x	detection	zoom	check scene	adjust magnification	x	
adjust magnification	x		x	x		x			placement	zoom	check scene	look	x	
look (glimpse)	x		x	x		x			adjustment	zoom	evaluate	decision	x	
target identified	x		x	x	x	x	x		match	zoom	verbal	test completed	x	
center target image	x		x	x		x		x	off-center	zoom	rotate head	adjust magnification	x	
sound cue-														
judgment		x	x	x	x				sound-cue	earphones	evaluate	decision	x	
align on cue			x	x				x	localizing	recall	rotate head	continue task	x	x
scene shift														
check sickness	x		x	x	x				motion	internal	evaluate	decision	x	
align view on scene	x	x	x	x	x	x		x	active	direct/HMD	rotate head	continue task	x	x

8

supervisory levels; and motor with ocular, vocal, and manual modalities. The operator interfaces include the event that elicits the sub-task, the interface display pertinent to the task, the feedback from the operator, and the ensuing action. Finally, the table lists the impact of the task performance on the maintenance of the mental model at both the task level and that of the global SA.

3.3   Task Information Processing

In this section of the report, we review a descriptive model for human information processing appropriate for the target detection and identification tasks. In the following section, a mental model and production rules are discussed for the tasks.

3.3.1 Task-Directed Behavior

Task-directed behavior may be thought of as composed of hierarchical components: a sequential activity for task performance and an accompanying assessment activity used to maintain a mental model of the process. The mental model (Norman, 1988) contains a knowledge-based understanding of the task and SA. The task sequence consists of skill-level behavior, which is directed by a rule-based script type schema (Brookhuis, De Vries, & De Waard, 1991) developed for the particular problem from the mental model. An awareness of the surrounding problem structure is maintained to compose the schemas needed as new problems arise. As noted by Endsley (1993a, 1993b, 1996), this awareness can occur in the individual at several levels. These levels are (1) awareness of the problem, (2) knowledge of the problem class derived from pattern matching and the state of the elements comprising the problem structure for that class, and (3) an assessment of the consequences and a mapping of the problem and the elements to an appropriate solution scheme. Thus, SA is determined by the knowledge of the operator and his understanding of goals and tactics (Selcon, Taylor, & Koritsas, 1991).

The maintenance of a mental model and the accompanying SA is necessary for the continual planning of problem involvement and itself constitutes a form of secondary task with its own unique workload requirements. For this reason, problem solving is composed of dual tasks, which, while competing for attentional resources, consist of a sequential activity focused on a particular problem and an accompanying maintenance of SA of the problem environment. Performance is improved when the task demand is matched by the supply of knowledge and central processing resources in the human. Central processing may be conceived as drawing upon the cognitive resources according to the level of processing involved; that is, skill-, rule-, or knowledge-based behavior (Rasmussen, 1983, 1986, 1993). Here, skill-based behavior provides the task performance, rule-based behavior provides the governing schema for skill control, and knowledge-based provides the schema formation for the next task problem. Workload and awareness are related since attentional resources are used to acquire and maintain awareness. In turn, awareness of the task situation is needed for effective decision making and implementation. As with any task, awareness of the situation is limited by the attention capacity of the human (Wickens, 1992). The implication is that models of human information processing should include

9

a component in memory which is specialized for SA and a mental model of the task problem process (Gordon, 1997). Further, the model should include the attentional demands of complex decision making and problem solving which are used to maintain SA.

3.3.2 Mental Model

Table 2 lists a mental model for the detection and identification task in terms of goals and actions. In particular, the table lists the goals, operators, methods, and selection rules that could be used in a goals, operators, methods, and selection rules (GOMS) model of the task (Card, Moran, & Newell, 1983; Kieras, 1988). In this formulation, the human gunner has goals that are achieved by specific methods and selection rules. A method is defined as a script sequence of steps that are performed by the perceptual, cognitive, and motor operators. There are usually several methods that need to be performed to accomplish a goal. Selection rules are used to specify the conditions that must be satisfied for a method to be executed (Wickens, Gordon, & Lui, 1998).

Associated with the selection rules are parameters and features used in the decision making process. Table 3 lists a reference frame that would be held in memory for the parameters and features used with the selection rules of the detection task. The reference values are the values of the features used for the selection criteria. In the gunner's model, the mental model reference frame is part of working memory with the features values being filled by the perceptual processors as the task is executed. The reference values are established during training. The rule-based processor calls the selection rules according to the task script as each rule is processed in turn. Associated with each selection rule is the set of features and reference values used in processing.

3.3.3 Task Production Rules

The selection rules for the detection and identification task are in the form of conditional production rules that are processed by the rule-based processor. As listed in Table 4, the production rules are in an "if-then" format in which actions are activated (i.e., "fired") when the conditions of the parameters are satisfied. The rules are written in a C-language format with the function calls referring to perceptual and autonomous skill-based processor-driven motor activities.

3.3.4 Intrusive Task Production Rules

Table 5 lists production rules for the intrinsic tasks. By itself, body movement relative to the visual scene causes the participant to momentarily evaluate his mental model of his position in the scene. As shown in Figure 3, body movement imposes an additional sub-task in the SA domain that is time shared with the procedures of the structured task. However, vehicular motion may lead to inactivity because of motion sickness. In this process, motion sickness forces a monitoring of discomfort awareness as a secondary task competing for attentional resources. In some cases, motion sickness dominates the responses, causing the participant to momentarily

discontinue the primary task. Although the effect of total severity may be interpreted as the imposition of additional stressors that act as performance-shaping functions for the allocation of attention to the monitoring sub-task, the corresponding symptoms may have masking effects on the separate attention-processing channels. In this sense, the symptoms of motion sickness are degrading processing channels. For example, the oculomotor symptom may interfere with the visual processing channel, while the disorientation symptom may interfere with the cognitive channel through the impact on SA, and finally, the nausea symptom may appear to be an added attention loading on an activated somato-sensory channel that is otherwise dormant.

Table 2. Mental Model of Target Detection and Identification Tasks

---

Goal - Find target on the experimental facility and identify as quickly as possible.

Operators - Visually search and identify by direct vision or with head-controlled telescopic camera using eye and head movements, manual manipulation of binoculars or telescopic zoom control, and voice responses.

Method - Following verbal directive from experimenter, start search over front of experimental facility with direct vision or head-controlled telescopic camera. Inform experimenter when target is located. Depending on the search method, raise binoculars to face or increase telescopic zoom and focus on target to determine orientation of target marker, and inform experimenter.

Selection rules - The rules used by the participant in executing the method:

  (1) The experimenter informs the participant when the trial is to start.

  (2) The target is a human silhouette on an experimental facility in the right front sector from 50 meters to 250 meters.

  (3) Direct vision or an HMD may be used in the search and identification processes; the vehicle from which the search is made may be stationary or moving along side the range; and a localization sound apparently emitting from the direction of the target may be presented throughout the search period.

  (4) The search is conducted in a sequence of visual glimpses, starting at the front and proceeding to the right until the sector side is reached.

  (6) Once the target is sighted, a verbal response of "target sighted" should be made to the experimenter, and identification should commence.

  (7) In the identification procedure, the visual field of a pair of binoculars or of the HMD should be centered on the target and the field zoomed on the target by manual adjustment until the identification marker can be seen.

  (8) The identification marker is a Landolt C-ring on the face of the target with the ring gap oriented up, down, right, or left.

  (9) Upon identification, a verbal response "up," "down," "right," or "left" describing the ring orientation should be made to the experimenter.

  (10) The trial ends with the identification response or when the experimenter so commands.

Table 3. Frame of Reference

Parameter	Features	Reference Values
Trial status	start	START_TRIAL
	target search	SEARCH
	detection made	TGT_DETECTED
	detection response	1st_VOICE_RESPONSE
	target image magnification	ZOOM_IMAGE
	identification made	TGT_IDENTIFY
	identity response	2nd_VOICE_RESPONSE
	end	END_TRIAL
Vehicle status	stationary	STATIONARY
	moving	MOVING
Search method	direct vision	DIRECT_VIEW
	HMD	HMD
Identification method	binoculars	BINOCULARS
	telescopic zoom	TELESCOPIC
Cueing method	none	NO_CUE
	sound localization	3D_AUDIO
target status	presented	TGT_PRESENT
	none	NO_TGT
Target	shape	HUMAN_SILHOUETTE
Target location	place	viewing sector
Detection response	verbal	"target detected"
Marker	shape	LANDOLT_C-RING
Marker feature	gap orientation	UP, DOWN, LEFT, RIGHT
Controller status	visual field zoom	ZOOM_LEVEL
Identity response	verbal	"Oriented up (down) (left) (right)"
Vehicle position	relative	viewing sector
Vehicle orientation	relative	viewing sector
Vehicle speed	optical	flow field
Scene texture	scene blob shape, size, color	terrain features
Velocity flow field	displacement of terrain texture	FLOW_SEPARATION
Body awareness	motion sickness	NONE, SICK, INCAPACITATED
Eye orientation	relative	head
Head orientation	relative	vehicle
Audio cue status	on	CUE_ON
	off	CUE_OFF
Audio cue response	respond	ORIENT
	ignore	SUPPRESS
Trial start	verbal command	"target up"
Trial end	identity response	verbal
	verbal command	"end trial"

Table 4. Production Rules for Target Detection and Identification Tasks

```
// detection:
inactivity: // wait for trial to start

if( hear("target up")) process_glimpse();
else
goto inactivity;

process glimpse()
{
glimpse();
if(beyond_FOV(Search_method))
    {   index_head();
        reset_eyefield();
        if(beyond recall(course)) {
            reverse_head();
            index_head();
            reset_eyefield(); } }
else index_eyefield();
process_glimpse();
}

glimpse()
{
blob_scene();
if(image_blob maps_to recall(target_shape))
    {voice_tell ("detection");
    goto identify; }
}

// identification::

identify:
if(direct_vision) place_binoculars();

continue_ID:
if(voice_tell("stop"))stop();
if(on_target != TRUE) orient_on_target();
adjust_zoom();
blob_scene();

if(image_blob maps_to recall(C_ring)) {
  decision(gap_orientation);
  voice_tell (gap_orientation);
stop();   }
else
goto continue_ID;
```

Table 5. Production Rules for Intrusive Tasks

```
// sound cue intrusion:

sound_cue()
{
decision();

if(decide == respond)
    {
    localize_on_cue();
    align_head();
    }
else
    {
    suppress();
    }
    return(); }
}

// body movement intrusion:

body_movement()
{

if(discomfort_aware() == sickness)
somatic_response();
else
place_self(vehicle,range);

}
```

Note: All function calls are at perceptual processors or autonomous skill level.

3.4 Summary of Statistical Results

The results of the field study are that more targets were detected with direct viewing than with the HMD and from the stationary position than the moving vehicle. Although more targets were detected with direct viewing from the stationary vehicle without cueing, sound localization improved target detection in all other treatments. Similar comments apply to identification from the stationary position; however, fewer targets were identified from the moving vehicle with sound localization than without. The advantages of auditory cueing for target detection may have been limited by the choice of an intermittent tone for sound localization and the restricted search sector used in the experiment.

Ratings of task attention loading show that increased attention was needed for the detection task with sound localization, especially with the HMD. This is also true for the identification task. Workload test battery ratings show a significant increase in perceived workload with the HMD as compared to the direct vision. A test of SA shows significant effects with decreasing trends in perceived stability and familiarity and an increased need to concentrate when one is using the HMD in the moving vehicle. Further, most of the participants reported a general discomfort

associated with motion sickness while in the moving vehicle with the HMD. There was no significant change in heart rate, with test mode indicating no impact of metabolic work on their performance. As a result of the study, the participants rated direct viewing as more useful than the HMD and the sound localization as being of more use with the HMD than with direct viewing.

3.4.1 Statistical Values of Measures

For modeling workload, the statistical values for the perceived workload, attention allocation, SA, and motion sickness are of interest. Table 6 lists the averages and standard deviations for the statistically significant mental workload measures as a function of the pertinent treatments. These measures are for the questionnaires on Task Loading Index (TLX), motion sickness, and Situation Awareness Rating Technique (SART), described in greater detail along with the attention allocation questionnaire, further in the report. The maximum possible scores are listed for reference. Note that the SART supply measures are considered to be insignificant by treatments. Table 7 lists the average scores for the statistically significant attention allocation factors for the detection and identification tasks. The equivalent verbal anchors are listed, along with the scores for reference. Note that the maximum possible allocation score on an attention channel is 7.

Table 6. Statistically Significant Mental Workload Questionnaire Results

Measure	Average	SD	Number
Total TLX:			
Direct viewing	13.966	9.958	32
HMD viewing	28.100	11.011	32
Motion Sickness Severity:			
All other cases	4.414	6.776	58
HMD & motion	22.199	23.342	16
SART measures:			
(a) Demand:			
Direct viewing	8.225	4.279	32
HMD viewing	11.538	4.614	32
(b) Supply:			
Arousal	3.362	1.735	64
Capacity	3.933	1.853	64
Concentration	4.586	1.497	64
Division	3.753	1.811	64
(c) Understanding:			
Direct viewing	14.672	3.924	32
HMD viewing	12.216	5.284	32

SD = standard deviation

Table 7. Statistically Significant Attention Loading Factors

Configuration	Number	Average Value[a]	SD	Verbal Anchor
I. DETECTION TASK				
(a) Visual channel:				
All treatments	64	3.575	2.190	"discriminate"
(b) Cognitive channel:				
All treatments	64	3.367	1.598	"recognize"
(c) Audio channel:				
Non cueing treatments	32	0.062	0.354	"none"
Sound cueing treatments	32	3.293	1.574	"orient," "verify"
(d) Psychomotor channel:				
Direct vision	32	1.788	1.538	"toggle"
HMD vision	32	3.781	1.519	"continuous," "manipulate"
II. IDENTIFICATION TASK				
(a) Visual channel:				
All treatments	64	3.973	1.957	"inspect"
(b) Cognitive channel:				
All treatments	64	3.667	1.916	"recognize"
(c) Audio channel:				
Non cueing treatments	32	0.000	0.000	"none"
Sound cueing treatments	32	2.725	1.683	"orient," "verify"
(d) Psychomotor channel:				
All treatments	64	3.039	1.880	"continuous"

[a]Note: maximum possible value on all channels equals 7.

4. Task Performance Model

A model is developed by regression analysis for the time to detect, the detection event, the time to identify, the identification event, and the correct identification from the experimental data.

4.1 Time to Detect

Given that the target is visible, the time to look at the target is the time to shift the gaze direction from the range front to the location of the target. The search strategy is one of shifting a visual search lobe across the visual front by a sequence of rapid eye movements integrated with intermittent head movements. The rate of shifting the search lobe is determined by the time for the human to (a) acquire a visual image for each lobe fixation, (b) perceptually isolate pertinent features from the image, and (c) cognitively compare the features to a physical template for the

target. Given a self-paced search task, this is an integrated activity of pipelined visual, perceptual, and cognitive processes.

In natural vision, the size of the search lobe is determined by the expected conditions for the target size and background; the search rate is determined by the angular size divided by the processing time. The search rate is lower for the HMD, since the angular size of the search lobe is reduced by the restricted view of the camera. Furthermore, the processing time is increased by the need to cognitively relocate the viewing direction on the course as the vehicle moves forward.

The sound cue narrows the search sector by orienting the participant toward the target. In the case of direct viewing, the search lobe is naturally wide, and the synthetic stereophonic process proved to be perceptually insensitive for the limited search sector. In contrast, the FOV of the HMD is narrower than the cued sector. In this case, while sound localization initially orients the participant toward the target, this is followed by a refined visual search.

Further, sound localization bypasses the visual processor and involves the human acoustic processor for signal isolation, the cognitive processor for comparing the stereophonic signals, and ocular and head motor adjustment to align the signals. In practice, because of the intermittent tone and limited search sector used in this experiment, the sound localization may have increased the processing time by adding to the visual task. The intermittent tone caused the participant to momentarily wait between tones to make adjustments, and visual processing occurred during the off-duty cycle.

For these reasons, the time to detect (t_d), given a detection, is the angular separation (ϕ_E) of the target from the participant's initial orientation divided by the size of the search lobe (ϕ_Σ), multiplied by the inverse of the rate of search. Without cueing, the separation angle is the angle of the target from the range front (ϕ_T). With cueing, the angle is for orientation (ϕ_X). The search lobe size is different for direct viewing and the HMD. The inverse rate of search is represented by a natural vision constant (K_0) multiplied by adjustments for the treatments of vehicular motion (a_m), use of the HMD (a_v), and considering the statistical results, by the interaction of the sound localization with the motion and vision modes (a_s). The detection time is

$$t_d = t_s + [K_0 * a_m * a_v * a_s] * \phi_E / \phi_\Sigma,$$

in which the adjustments are unity for those cases when the treatment conditions do not apply. A fixed time component, t_s, has been added to account for the reaction times of the participant to the verbal command to start the trial, the participant to verbally respond to his sighting, the experimenter to the verbal response, and the facility control to the experimenter's flag. Taking the natural logarithm of both sides, we have the linear expression,

$$\ln(t_d - t_s) = \beta_0 + \beta_m * \alpha_m + \beta_v * \alpha_v + \beta_s * \alpha_s + \beta_T * \ln(\phi_E / \phi_\Sigma),$$

in terms of the effects coding (α = 0 or 1) for the treatments and the corresponding powers (β) of the natural exponential as regression coefficients. Here, a coefficient has been included for the target angle; the viewing lobe is assumed fixed in size. A stepwise linear regression fit of the equation to the detection times for those targets detected is statistically significant (adjusted R-square = 0.399, p < .001, F = 113.292, df = 3, dfe = 504), with significant coefficients for the vehicle motion (b_m = 0.156, p < .001) and viewing with the HMD (b_v = 0.587, p < .001), and the interaction with sound localization excluded by the analysis. The vehicle motion and HMD both increase the time to detection. However, while the regression coefficient for the target angle is significant (b_T = 0.156, p < .001), the value is much less than unity. The detection times are increased for the targets near the extreme edge of the search sector but not for those toward the range front or between. This implies that the search sector (60 degrees) was too narrow to force different search strategies for the different treatments except at the extreme target angles.

4.2 Detection Event

The detectability of a viewed target is a direct function of its visibility. For a distant outdoor target, the visibility is a function of its shape, apparent area, range, and brightness contrast. Additional factors are the viewer's visual acuity and adaptation brightness. For outdoor viewing, the brightness contrast is determined by the sun angle relative to the viewing direction and the reflectance of the target and its surroundings (Smyth, 1988). The target range used in this study is oriented in the east-west direction, and all viewing was toward the east. Experimental trials were performed from 10 a.m. to 2 p.m. to ensure an overhead sun.

Given that the participant is looking at the target, detection occurs if the visibility of the target exceeds a threshold value. The effective area is the true area adjusted by the cosine of the target angle to the observer. The HMD may reduce the visibility because of the reduced resolution of the display. Similarly, vehicle motion reduces the resolution by motion blurring of the image. Sound localization may effectively increase the visibility by increasing the participant's signal detection sensitivity; however, the statistical results show no such effect. Furthermore, the statistics show dependency upon the interaction between the HMD and vehicle motion. For daytime viewing, we assume that the adaptive brightness is constant. For these reasons, the visibility (V_T) is the product of adjustments for the vehicle motion (a_m), use of the HMD (a_v), and the interaction between the two (a_{mxv}), along with the target area (A), cosine of the target angle (ϕ_T), brightness contrast (b_c), and visual acuity (a_c) of the participant, all divided by the square of the target range (ρ_T). That is,

$$V_T = K_o * a_m * a_v * a_{mxv} * a_c * b_c * A * \cos(\phi_T)/\rho_T^2.$$

Taking the natural logarithm of both sides, we have the linear expression

$$\ln(V_T) = \beta_0 + \beta_m * \alpha_m + \beta_v * \alpha_v + \beta_{mxv} * \alpha_{mxv} + \beta_T * \ln[a_c * b_c * A * \cos(\phi_T)/\rho_T^2],$$

in terms of the effects coding (α = 0 or 1) for the treatments and the corresponding powers (β) of the natural exponential. Here, a coefficient has been included for the target visibility.

18

Considering a discriminant function (D_T) which is unity for a successful detection and zero for a failure to detect, a stepwise regression analysis of the target detection is significant (adjusted R-square = 0.366, $p < .001$, F = 148.268, df = 3, dfe = 762), with significant coefficients for viewing with the HMD ($b_v = -0.343$, $p < .001$) and motion with the HMD ($b_{mxv} = -0.227$, $p < .001$), with however, the vehicle motion excluded. As expected, the HMD and motion with the HMD both decrease the target visibility. However, while the regression coefficient for the target visibility is significant ($b_T = 0.149$, $p < .001$), the value is much less than unity; the detection events are decreased by the targets near the far range of the search sector but not by those that are close or between.

4.3 Time to Identify

Once the target has been detected, the time to identify is the time that the participant needs to magnify the target image so that the Landolt ring gap is visible. The time is a function of whether binoculars or electronic zooming is used. Also, vehicular motion reduces resolution by blurring the image. However, since the image has been located, sound localization provides no assistance if visual focus on the image is maintained. According to the statistical results, the interaction of the vehicle motion with the HMD has an effect. Another factor is the target range since a distant target will have to be viewed at a higher magnification for the identification marker to be seen. Furthermore, the gap area (A_g) seen is a function of the cosine of the target angle, ϕ_T. Also, the participant's visual acuity determines the magnification level needed to see the marker image. In this case, the brightness contrast is not a factor since it is fixed for the marker on the target board. The adjustment will take longer for those targets that need to be seen at a higher magnification. The expression for the identification time including the response times, is

$$t_{id} = t_s + K_o * a_m * a_v * a_{mxv} * [\rho_T^2/(a_c * A_g * \cos(\phi_T))].$$

Taking the natural logarithm of both sides, we have the linear expression

$$\ln(t_{id} - t_s) = \beta_o + \beta_m * \alpha_m + \beta_v * \alpha_v + \beta_{mxv} * \alpha_{mxv} + \beta_T * \ln[\rho_T^2/(a_c * A_g * \cos(\phi_T))],$$

in terms of the effects coding ($\alpha = 0$ or 1) for the treatments and the corresponding powers (β) of the natural exponential. A stepwise linear regression fit of the equation to the identification times for targets identified is significant (adjusted R-square = 0.182, $p < .001$, F = 28.563, df = 3, dfe = 368), with significant coefficients for the vehicle motion ($b_m = 0.113$, $p < .001$) and viewing with the HMD ($b_v = 0.109$, $p < .001$), with the interaction excluded. As expected, the vehicular motion and use of the HMD increase the time to identify. As before, the regression coefficient for the target is significant ($b_T = 0.076$, $p < .001$). Since the value is much less than unity, the identification times are increased by the targets that are near the far range of the search sector.

19

4.4 Identification Event

Given that the participant is looking at the Landolt ring, identification occurs if the visibility of the ring gap exceeds a threshold value; however, it is assumed that the participant has magnified the image to a level exceeding this threshold. In this case, the identification is a function of the visual and vehicular motion treatments and the interaction. That is,

$$V_T = K_0 * a_m * a_v * a_{mxv}.$$

Again, taking the natural logarithm of both sides, we have the linear expression

$$\ln(V_T) = \beta_0 + \beta_m * \alpha_m + \beta_v * \alpha_v + \beta_{mxv} * \alpha_{mxv},$$

in terms of the effects coding ($\alpha = 0$ or 1) for the treatments and the corresponding powers (β) of t he natural exponential. Considering a discriminant function (D_T), which is unity for a successful identification and zero for a failure to identify, a stepwise regression analysis of the target identifications for those targets detected is significant (adjusted R-square = 0.309, $p < .001$, $F = 114.131$, df = 2, dfe = 505), with significant coefficients for vehicular motion ($b_m = -0.105$, $p < .002$), and viewing with the HMD ($b_v = -0.530$, $p < .001$), with the interaction excluded by the analysis. As expected, the vehicular motion and use of the HMD decrease the identifications.

4.5 Correct Identification

A similar argument applies to the incidents of correct identification for those targets identified. A regression analysis of the correct identifications is significant (adjusted R-square = 0.109, $p < .000$, $F = 46.476$, df = 1, dfe = 370), with significant coefficients for the vehicular motion ($b_m = -.306$, $p < .001$) but not for viewing with the HMD, which is excluded. As expected, the vehicular motion decreases the incidences of correct identification.

---

5. Mental Workload Measures

While the task model developed previously describes the task performance, the mental workload is of interest since it can influence performance. Over long periods of time, excessive mental loading can lead to fatigue and consequently slow responses and increase errors. Furthermore, increased mental workload can result in a loss of SA for other problems, which can impact future decision making. Discussed are the mental workload measures as determined by the relation between the perceived task workload and the attention allocation, SA, and motion sickness. The relationship among the measures is analyzed, and the dependency of the perceived workload on the other mental workload measures is determined. We start with a discussion of task-directed behavior and an interpretation of the workload measures in behavioral terms. This approach follows a procedure developed to model workload for indirect vision driving (Smyth, 2002a).

20

5.1 Workload Measures

The mental workload measures used in this study are the product of the previously mentioned field experiment (Smyth, 2002b), during which, subjective evaluations were collected as completed questionnaires from the participants at the end of each block of trial runs.

5.1.1 Mental Workload Questionnaires

The questionnaires applied in the field experiment are as follow.

5.1.1.1 NASA TLX

The National Air and Space Administration (NASA) TLX workload questionnaire (Hart & Staveland, 1988) is used for rating the perceived workload in terms of task demand and interaction. The NASA-TLX is a multidimensional rating procedure for the subjective assessment of workload. The developers of the questionnaire have defined workload as a hypothetical construct that represents the cost incurred by the human operator to achieve a specific performance level. The construct is composed of behavioral, performance, physiological, and subjective components that result from the interaction between a specific individual and the demands imposed by a particular task. The questionnaire consists of six 9-point (0 to 9) bipolar scales for rating the mental, physical, and temporal demands of the task and the effort, performance, and frustration of the participant (Charleton, 1996).

5.1.1.2 Allocation of Task Attention

The questionnaire is used for rating the allocation of attention to the visual, auditory, cognitive, and motor processing channels of the human operator according to loading factors (McCracken & Aldrich, 1984). These loading factors are used in task analysis workload (TAWL) simulations (Allender, Salvi, & Promisel, 1998). The questionnaire consists of a set of four 7-point (0 to 7) bipolar scales for rating the attention loading on each channel, with verbal anchors for corresponding activities overlaid on the scales.

5.1.1.3 SART

The SART questionnaire, which is used for rating the SA (Taylor, 1988, 1989; Taylor & Selcon, 1994; Selcon, Taylor, & Koritsas, 1991) was designed to measure subjective ratings of non-attentional factors such as domain knowledge or schemata and experience, the cognitive nature of the information received while the task is being performed, and the workload needed to process the information. The questionnaire consists of ten 7-point (1 to 7) bipolar scales for rating the dimensions of assessment demand, ability, and knowledge. In this study, we refer to SA as the participant's awareness of the location of his experimental vehicle on the targeting course during a trial run.

5.1.1.4 Motion Sickness

The motion sickness questionnaire is used for the subjective estimation of motion sickness (Kennedy, Lilienthal, Berbaum, Baltzley, & McCauley, 1989). The questionnaire lists 4-point (0 to 3) bipolar rating scales consisting of verbal descriptors for the 16 symptoms such as general discomfort, eye strain, dizziness, and nausea. Based on data from a factor analysis of simulator sickness experiences, a procedure has been developed (Kennedy, Lane, Lilienthal, Berbaum, & Hettinger, 1992) for reducing the scores to subscales for the symptomatic components of oculomotor stress (eye strain), nausea, and disorientation, and in turn, a measure of total severity.

5.1.2 Behavioral Interpretation of Measures

The perceived workload is the result of the attention devoted to the separate mental functions needed in targeting. These are the needs for allocating attention to the targeting task, maintaining SA, and monitoring for motion sickness. The perceived workload is the mental workload imposed on the participant in the experiment. The workload measure consists of demand and interaction dimensions. Although demand dimensions separately rate the perceived levels of the perceptual, mental, and physical loading experienced by the participant, the interaction dimensions rate the perceived success of the control applications. In the following, an argument is presented for the measures describing different mental functions that impact perceived workload. Perceived workload is interpreted as the product of the other measures: task attention loading, associative processing for SA, and the monitoring of the somatic state of motion sickness. This interpretation follows from a review of the questionnaires, the results of which are presented as follows:

5.1.2.1 NASA TLX

The perceived workload is the workload imposed on the operator by his or her participation in the task. While the demand dimensions refer to the perceptual, mental and physical components of task involvement, the interaction dimensions refer to the levels of evaluation needed.

5.1.2.2 Attention Allocation

The ratings describe the attention that needs to be applied to the human information processors (i.e., channels) to perform the task. These are the vision and auditory perceptual processors, the cognitive processor and the psychomotor processor. While the perceptual processors concern association and encoding of stimuli, the cognitive processor evaluates and selects actions through working memory. The psychomotor processor executes the actions selected. However, a review of the rating anchors used in this study suggests that the ratings are limited to the performance of well-learned sequential tasks such as selecting a radio frequency while flying an aircraft (McCracken & Aldrich, 1984). In general, the working memory of the cognitive processor can be involved in more engaging tasks, such as selecting courses of action from long-term memory (Warwick, McIlwaine, Hutton, & McDermott, 2001).

5.1.2.3 SART

The questionnaire judges the ease with which environmental cues can be assimilated into the mental model of the task structure. The demand dimensions describe the perceptual nature of the cues, the number of variables, the complexity of the relations among them, and how quickly the relations are changing. These dimensions determine the perceptual attention needed to track the cues and associate them with the elements of the task mental model. The supply dimensions describe the mental capacity available to process the perceived cues. This capacity is determined by the alertness, the spare mental capacity available, the concentration demanded by the task being performed, and the distribution of attention among competing tasks. The understanding dimensions describe the ease with which these cues are assimilated with the mental model as determined by the information associated with the cues and with prior experience. Essentially, an environmental cue that cannot be easily assimilated into the task mental model will provoke a focus of attention onto the cognitive processor for further study and evaluation.

5.1.2.4 Motion Sickness

The questionnaire rates the attention dedicated to the somatic channel that is induced by the occurrence of motion sickness symptoms. As has been noted, while mild motion sickness results in discomfort, extreme cases can arrest operant behavior, causing the primary task to be momentarily discontinued while full attention is focused on the somatic state.

5.2 Analysis of Mental State Measures

We analyzed the mental workload measures for significant groupings of the measure dimensions. It is argued that the application of a factorial analysis to the mental workload measures constitutes a cognitive loading space, which, following rotation, forms a "skills-rules-knowledge" information processing space. The dependency of the perceived workload dimensions on the SRK components is analyzed and discussed.

5.2.1 Statistical Relationships Among Measures

Table 8 is a correlation matrix for the dimensions of the mental workload measures. Because many of the distributions are non-parametric, the correlation entries are computed with the bivariate Spearman-rho statistic. The table shows in bold lettering the entries that are significant at the $p < 0.01$ level (two-tailed test). Using this level of probability as a lower boundary, we consider first the interrelations among the dimensions of the measures and in turn, the intra-relations among dimensions between measures.

Table 8. Spearman-rho Correlation Matrix for Mental Workload Measures

		Mental	Physical	Temporal	Effort	Performance	Frustration	Visual	Cognitive	Auditory	Motor	Visual	Cognitive	Auditory	Motor	Instability	Variability	Complexity	Arousal	Mental Capacity	Concentration	Attention division	Info Quantity	Info Quality	Familiarity	Oculomotor	Nausea	Disorientation
		TLX Demand			**TLX Interaction**			**Detection Channels**				**Identification Channels**				**SART Demand**			**SART Supply**				**SART Understanding**			**Sickness**		
TLX	Mental	1.0	.522	.709	.494	.750	.666	-.324	-.229	.066	-.157	-.189	.073	.163	-.174	.610	.478	.628	.531	.183	.614	.457	.026	-.138	-.607	.258	.359	.184
	Physical		1.0	.620	.326	.502	.575	-.110	-.089	.430	-.250	-.102	.003	.523	-.305	.578	.408	.462	.647	.309	.298	.357	.228	.198	.064	-.132	.300	-.146
	Temporal			1.0	.439	.771	.703	-.144	-.132	.185	-.216	-.071	-.004	.282	-.120	.598	.460	.430	.701	.358	.566	.455	.084	-.028	-.388	-.036	.352	-.067
	Effort				1.0	.486	.667	-.129	-.116	-.177	-.050	-.455	-.199	-.047	-.148	.339	.168	.423	.201	-.216	.570	.284	-.158	-.226	-.543	.291	.434	.240
	Performance					1.0	.737	-.214	-.206	.168	-.140	-.085	.009	.245	-.060	.716	.461	.633	.632	.215	.602	.485	-.016	-.115	-.484	.153	.371	.043
	Frustration						1.0	-.097	-.080	.268	-.048	-.255	-.065	.338	-.144	.503	.228	.491	.494	.045	.535	.285	.170	-.223	-.386	.042	.330	-.036
Detection Attention loading	Visual							1.0	.624	.092	.138	.401	.312	.145	.087	-.212	-.151	-.280	-.123	-.042	-.120	-.242	.188	-.131	.392	-.216	-.231	-.174
	Cognitive								1.0	.097	.103	.393	.610	.115	.023	-.144	-.050	-.194	-.124	-.149	-.083	-.142	-.112	-.072	.254	-.266	-.196	-.175
	Auditory									1.0	.167	.115	.088	.881	-.005	.121	.029	.166	.384	.324	.096	.094	.169	.311	.413	-.246	.025	-.206
	Motor										1.0	.245	.316	.095	.669	.312	-.289	-.204	-.131	-.147	.090	-.168	-.119	.053	.063	-.007	-.203	.028
Identify Attention loading	Visual											1.0	.577	.075	.301	.000	.079	-.080	.046	.049	-.174	-.061	.026	.050	.232	-.184	-.286	-.130
	Cognitive												1.0	.098	.134	.123	.199	.035	.100	.011	.056	.105	.101	.114	.094	-.052	-.061	.019
	Auditory													1.0	-.087	.152	.027	.210	.391	.320	.153	.097	.123	.220	.310	-.144	.145	-.082
	Motor														1.0	-.276	-.287	-.231	-.101	-.011	.088	-.133	-.171	-.060	.048	-.105	-.268	-.082
SART	Instability															1.0	.714	.714	.714	.213	.452	.507	.275	.124	-.252	.052	.274	-.006
	Variability																1.0	.582	.486	.062	.340	.719	.386	.323	-.200	.214	.301	.132
	Complexity																	1.0	.498	.018	.531	.494	.121	.075	-.399	.155	.253	.040
	Arousal																		1.0	.459	.568	.454	.506	.401	.010	-.083	.266	-.108
	Mental Capacity																			1.0	.200	.076	.223	.263	.174	-.330	-.120	-.311
	Concentration																				1.0	.524	.220	.112	-.372	.219	.351	.164
	Attention division																					1.0	.491	.424	-.246	.481	.503	.399
	Quantity																						1.0	.873	.326	.027	.188	.041
	Quality																							1.0	.419	.025	.105	.065
	Familiarity																								1.0	-.437	-.268	-.322
Sickness	Oculomotor																									1.0	.697	.934
	Nausea																										1.0	.662
	Disorientation																											1.0

Note: **Bold** correlation entries statistically significant at the p < 0.01 level (two-tailed test).

24

5.2.1.1 Perceived Workload

All dimensions of perceived workload are significantly correlated with each other. In turn, some workload dimensions are correlated with those of attention loading, SA, and the nausea symptom of motion sickness. In particular, all workload demand dimensions are correlated with the SART demand dimensions, all are correlated with some supply dimensions, and mental and temporal demand are correlated with the familiarity dimension and nausea. Further, the workload mental demand is correlated with visual loading for detection and with physical demand with the auditory channels. Similar comments apply to the workload interaction dimensions, with all these dimensions correlated with some of the SART demand, supply, and understanding dimensions, and with the nausea symptom. Effort is also correlated with visual identification, and frustration is correlated with auditory identification.

5.2.1.2 Attention Allocations

The visual channels are correlated with the respective cognitive channels, the identification cognitive channel with the visual detection, and all detection channels with the respective identification channels. In turn, the auditory channels are correlated with the SART arousal, the auditory detection also with the mental capacity and familiarity, and the visual detection with familiarity. However, none of the attention-loading dimensions are correlated with the motion sickness symptoms.

5.2.1.3 Situational Awareness

All demand dimensions are correlated with each other, as are all understanding dimensions. Arousal is correlated with the other supply dimensions and concentration with attention division. All demand dimensions are correlated with some supply dimensions, and some demand dimensions are correlated with understanding dimensions. Arousal correlates with information quantity and quality, concentration with familiarity, and attention division with information quantity. All supply dimensions except arousal are correlated with some sickness symptoms, and familiarity with the oculomotor symptom.

5.2.1.4 Motion Sickness

All symptoms are correlated with each other.

In summary, most of the measure dimensions from this study are correlated within a measure and across measures. The workload dimensions are correlated among themselves and with dimensions of attention loading and SA and with sickness symptoms. In turn, the attention loading factors are correlated with SART dimensions but not with sickness symptoms. Finally, SART dimensions are correlated with themselves and with the sickness symptoms.

5.2.2 Cognitive Component Space

Perceived workload is interpreted as the weighted sum of the attention to (a) the perceptual, cognitive, and psychomotor task-level processors; (b) the perceptual association and cognitive processing of situational cues; and (c) monitoring the somatic channel as induced by motion sickness. However, as has been noted before, the task allocation, SART, and motion sickness dimensions are intra-correlated. For this reason, the derivation of a unique expression for the workload by regression analysis with the stepwise method is difficult because of the collinearity between these measures. One technique commonly used is principal component expansion to reduce the measures to an orthogonal representation of the experimental variance and to perform a regression analysis on the resulting basic set (Neter, Kutner, Nachtsheim & Wasserman, 1996).

Figure 4 shows a factorial component loading diagram for the task allocation, SART, and motion sickness measures, following reduction to three components with a factor analysis with principal component expansion as the extraction method (55.53% total variance explained), and Varimax rotation with Kaiser normalization. Because of the high inter-correlation between dimensions, the SART dimensions for demand and understanding were reduced to the corresponding sums, and the symptoms were reduced to the total motion sickness. However, the SART-supply and task allocations show low inter-correlation, and the separate dimensions were used in the analysis. Table 9 lists the rotated component matrix for the factor analysis.

Table 9. Component Matrix

Measure	Factorial Component		
	First	Second	Third
SART			
Demand	0.842	-.115	0.092
Arousal	0.594	-.072	0.603
Capacity	0.101	-.166	0.669
Concentration	0.733	-.094	0.227
Division	0.846	-.082	0.078
Understanding	0.033	0.005	0.606
Motion sickness			
Total severity	0.583	-.087	-.335
Detection allocation			
Visual	-.291	0.617	0.133
Cognitive	-.128	0.768	0.073
Auditory	-.023	0.197	0.808
Motor	-.108	0.526	-.026
Identification allocation			
Visual	0.034	0.743	0.105
Cognitive	0.230	0.810	0.016
Auditory	0.043	0.160	0.805
Motor	-.163	0.426	-.075

5.2.3 SRK Processing Structure

One way of looking at the loading diagram is that it forms a cognitive component space with information processing defining a cognitive state trajectory through the space. Considering the groupings of the measures, it can be argued that the component axes correspond to levels of cognitive processing. In particular, we argue that the components correspond to the skills, rules, and knowledge levels of reasoning (Rasmussen, 1983, 1986, 1993). In Figure 4, Component 2 corresponds to the skills level, Component 1 to the rules, and Component 3 to knowledge reasoning. This interpretation is based on the following argument.
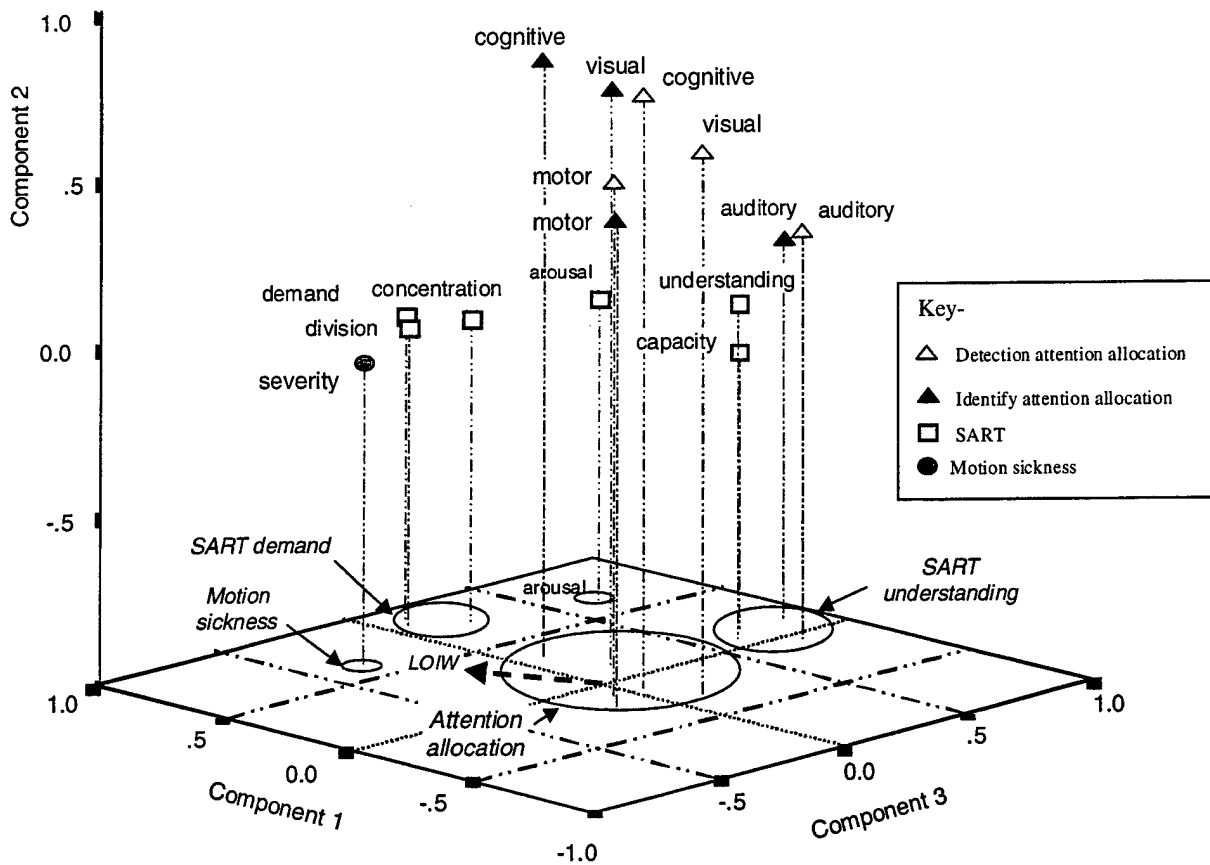
Figure 4. Cognitive Component Space.

Notice that the SART-understanding sum, which implies knowledge, projects to Component 3, with little projection to the other two components. Similarly, the SART-demand sum along with the supply concentration and division of attention, projects to Component 1, with little projection to the other two components. Here, considering the nature of the dimensions, cognitive demand implies rule-based analysis. Finally, visual and cognitive attention, which imply task focus, are predominantly aligned with Component 2, while SART and motion sickness, which imply internal focus, have little projection to this component. However, task focus in turn implies skill-based behavior.

27

This interpretation is supported by the fact that the projections of the attention allocation dimensions are clustered about the intersection of Components 1 and 3, implying that little rule-based or knowledge-based reasoning is used in the allocation dimensions. This is true of all but the two auditory dimensions, which are clustered with the SART-understanding sum, along with the SART-supply dimension of limited mental capacity. Notice that all SART values have minimal projection to Component 2, implying little skilled behavior. In turn, Figure 4 shows motion sickness with none of the skills of Component 2, negative knowledge or understanding from Component 3, and a direct rule response for Component 1.

5.2.4 Total Workload

Following the argument just given, the perceived workload is interpreted as a weighted sum of the attention applied to the three levels of reasoning. A correlation of the perceived workload with the factorial components via the non-parametric bivariate Spearman-rho statistic for a two-tailed test shows that the total TLX is significantly correlated with the first ($R^2 = 0.663$, $p < 0.001$, N = 64) and second ($R^2 = -.411$, $p = 0.001$, N = 64) components but not the third. The implication is that the total workload is determined by the attention demanded by the task allocation and the rules processing but not by knowledge processing for this task.

Applying curve estimation techniques for relating the workload to the factorial components, the total workload is described by a cubic polynomial with a constant term in the first component and a linear polynomial with a constant term in the second but not at all in the third. A linear regression analysis of the total workload as a function of the powers of the first and second factorial components with the entry method (Pedhazur, 1982) is statistically significant (adjusted $R^2 = 0.438$, $p < .001$, F = 13.256, df = 4, dfe = 59); however, none of the coefficients are significant. The entry method produces residuals that are uniformly distributed across component values.

The results of the analysis suggest that perceived workload for this study is a product of skill- and rule-based reasoning but not knowledge-based reasoning. In particular, the total workload index (TTLX) is given by

$$TTLX = -0.161$$
$$-0.165*SKILLS$$
$$+1.710*RULES - 3.119E\text{-}02*RULES^2 + 2.294E\text{-}04*RULES^3, \tag{1}$$

in terms of the first ("RULES") and second ("SKILLS") factorial components, with the coefficients in scientific notation. The factorial components are expressed as a weighted sum of the measures used in the analysis, and the corresponding weights are listed in Table 9. Following Equation (1), the isobars of constant workload form a family of curvilinear lines in the skills-rules plane (defined by Components 1 and 2). These isobars are perpendicular to the locus of increasing workload, which, for low component values, is practically at a $-5°$ angle to the rules axis (Component 1), as shown in Figure 4.

5.2.5 Statistical Values of Components

For modeling workload, the statistical contributions of the factorial components to the workload are of interest. Table 10 lists the averages and standard deviations for the contributions to the total workload from the first two components predicted with Equation (1), as a function of the experimental treatments collapsed across direct and HMD viewing. A study of the statistics for the contribution from the "SKILLS" component shows that the direct and indirect distributions for the contributions from the component are different; in particular, the mean for one distribution is not bound by the 95% confident interval for the mean of the other. Similarly, the direct and indirect distributions for the contributions from the "RULES" component are different; in particular, the mean for one distribution is not bound by the 95% confident interval for the mean of the other. The implication is that the significantly statistical change in workload with visual treatment is caused by the changes in both the SKILLS and RULES components.

Table 10. Significant Statistics for Total Workload Contributions From The First Two Factorial Components

| | | Treatment | | | | |
Component	N	Direct Average	SD	N	HMD Average	SD
SKILLS	32	14.076	17.519	32	-1.285	0.807
RULES	32	19.160	6.577	32	26.682	7.882

5.2.5.1 SKILLS Component

A study of Table 9 shows that the major sources of Component 2 are the task allocated attention to the visual, cognitive, and motor channels for the detection and identification tasks. Table 7 lists the statistics for these measures as a function of the experimental treatments. The table shows that the average loading for the detection task psychomotor channel is significantly increased by the HMD viewing. In contrast, the average loading values for the visual and cognitive channels are not significantly changed by the treatments for both tasks. This is true also for the identification psychomotor channel. Thus, the loading on the detection task psychomotor channel is the primary source of the significant change in the SKILLS component with viewing treatment.

5.2.5.2 RULES Component

A study of Table 9 shows that the major sources of Component 1 are the SART-demand, the SART concentration and division dimensions, and motion sickness severity. Table 6 lists the statistics for these measures as a function of the experimental treatments. The table shows that the average for the SART demand is significantly greater for the HMD while the average for motion sickness is significantly greater for the HMD in the moving vehicle. These variables are

the sources of the increase in the workload contribution from Component 1 for the indirect vision treatment.

5.2.6 Expected Total Workload

Using Equation (1) for the total perceived workload given previously, we may compute the average expected values from the data for each treatment. Figure 5 is a set of bar column plots of the average predicted total workload as a function of treatment conditions. The figure shows that the average predicted values for the direct viewing treatment are within or close to the 95% confidence interval for the statistically significant average of 13.966 for that treatment. Similarly, the average predicted values for the HMD viewing treatments designated by vehicular motion, are within or close to the 95% confidence intervals for the statistically significant averages of 26.431 for the stationary vehicle and 29.769 for the moving vehicle.
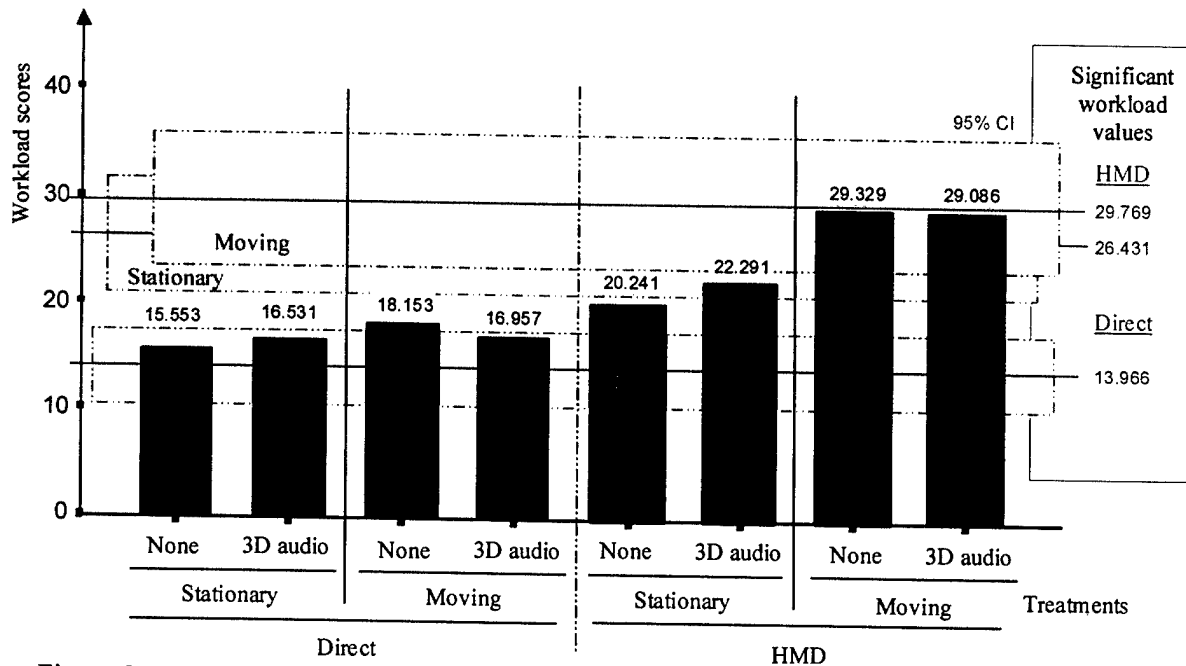
Figure 5. Average Predicted Total Workload for Treatment Conditions.

5.2.7 Workload Dimensions

The relations of the perceived workload dimensions to the factorial components are of interest. In this section, we present the results of statistical analyses for the separate dimensions of perceived workload.

5.2.7.1 Mental Demand

A correlation analysis with the non-parametric bivariate Spearman-rho statistic for a two-tailed test shows that the dimension is significantly correlated with the first ($R^2 = 0.583, p < 0.001$, $N = 64$) and second ($R^2 = -0.343, p = 0.006, N = 64$) components but not the third. When we apply curve estimation techniques, the mental demand is described by a cubic polynomial with a

constant term in the first component and a linear term in the second. A linear regression analysis of the dimension as a function of the powers of the factorial components via the entry method is statistically significant (adjusted $R^2 = 0.392$, $p < .001$, F = 11.160, df = 4, dfe = 59); however, none of the coefficients are significant. The unstandardized coefficients for the analysis are $b_0 = -0.020$, $b_1 = 0.197$, $b_2 = -5.867E-04$, and $b_3 = -5.550E-06$, for the first component, and $b_1 = -2.187E-02$ for the second, where the indices match the component power. The entry method produces residuals that are uniformly distributed across component values. The results of the analysis suggest that mental demand for this study is a product of skill- and rule-based reasoning but not knowledge-based reasoning.

5.2.7.2 Physical Demand

The dimension is significantly correlated with the first ($R^2 = 0.389$, $p = 0.001$, N = 64) component but not the second or third. The physical demand is described by a cubic polynomial with a constant term in the first component. A linear regression analysis as a function of the powers of the first factorial component is statistically significant (adjusted $R^2 = 0.272$, $p < 0.001$, F = 8.855, df = 3, dfe = 60); however, none of the coefficients are significant. The un-standardized coefficients for the analysis are $b_0 = -1.155$, $b_1 = 0.271$, $b_2 = -7.014E-03$, and $b_3 = 6.517E-05$. The results of the analysis suggest that physical demand is a product of rule-based reasoning but not skills or knowledge.

5.2.7.3 Temporal Demand

The dimension is significantly correlated with the first ($R^2 = 0.462$, $p < 0.001$, N = 64) component but not the second or third. The dimension is described by a cubic polynomial with a constant term in the first component. A linear regression analysis is statistically significant (adjusted $R^2 = 0.216$, $p = 0.001$, F = 6.794, df = 3, dfe = 66); however, none of the coefficients are significant. The unstandardized coefficients for the analysis are $b_0 = -0.161$, $b_1 = 0.310$, $b_2 = -5.479E-03$, and $b_3 = 3.667E-05$. The entry method produces residuals that are uniformly distributed across component values. The results of the analysis suggest that the temporal demand is a product of rule-based reasoning but not skills or knowledge.

5.2.7.4 Effort

The dimension is significantly correlated with the first ($R^2 = 0.478$, $p < 0.001$, N = 64) and second ($R^2 = -0.408$, $p = 0.001$, N = 64) components but not the third. The dimension is described by a cubic polynomial with a constant term in the first component and a quadratic polynomial in the second. A linear regression analysis is statistically significant (adjusted $R^2 = 0.293$, $p < 0.001$, F = 6.229, df = 5, dfe = 58); however, none of the coefficients are significant. The un-standardized coefficients for the analysis are $b_0 = 0.147$ for the constant, $b_1 = 0.509$, $b_2 = -1.299E-02$, and $b_3 = 1.033E-04$ for the first component, and $b_1 = -0.107$ and $b_2 = 3.908E-05$, for the second. The entry method produces residuals that are uniformly

distributed across component values. The results suggest that the effort is a product of the skill- and rule-based reasoning but not knowledge.

5.2.7.5 Performance

The dimension is significantly correlated with the first ($R^2 = 0.578$, $p < 0.001$, $N = 64$) component but not the second or third. The performance is described by a cubic polynomial with a constant term in the first component. A linear regression is statistically significant (adjusted $R^2 = 0.374$, $p < 0.001$, $F = 13.571$, df = 3, dfe = 60); however, none of the coefficients are significant. The un-standardized coefficients for the analysis are $b_0 = 0.302$, $b_1 = 0.159$, $b_2 = 5.537E-04$, and $b_3 = -1.788E-05$. The entry method produces residuals that are uniformly distributed across component values. The results of the analysis suggest that performance is a product of rule-based reasoning but not skills or knowledge.

5.2.7.6 Frustration

The dimension is significantly correlated with the first ($R^2 = 0.392$, $p = 0.001$, $N = 64$) component but not the second or third. The dimension is described by a cubic polynomial with a constant term in the first component. A linear regression analysis is statistically significant (adjusted $R^2 = 0.181$, $p = .002$, $F = 5.627$, df = 3, dfe = 60); however, none of the coefficients are significant. The un-standardized coefficients for the analysis are $b_0 = 0.061$, $b_1 = 0.282$, $b_2 = -5.910E-03$, and $b_3 = 4.914E-05$. The entry method produces residuals that are uniformly distributed across component values. The results of the analysis suggest that the frustration is a product of rule-based reasoning but not skills or knowledge.

In summary, the statistical analyses for the separate dimensions of perceived workload as a function of the factorial components interpreted as cognitive levels of reasoning agree with the experimental results reported in the literature. This is true since they demonstrate the increase in workload demand and interaction with use of the HMD (Smyth, 2002b). Application of the Holm simultaneous testing procedure (Neter, Kutner, Nachtsheim, & Wasserman, 1996) for control of the type I error shows that the separate regression analyses listed previously for the total workload and dimensions satisfy a family-wise 0.05 alpha level. The implication is that the separate analyses are not statistically significant by chance alone because of the multiple testing.

5.2.8 Implications for Task Modeling

The results suggest that perceived workload is a function of what is being interpreted as skill- and rule-based reasoning but not of knowledge-based reasoning. This is reasonable since knowledge of the target range and experimental procedure was learned by the participants at the start of the experiment and did not vary with treatments. It is interesting that while both the skill- and rule-based reasoning are different by treatment, the attention allocation ratings used in this study appear to map to the skills level. However, intense cognitive processing is necessary to support the rules processing and maintain the mental model that is needed for range targeting. One possibility is that rating forms did not include activities as anchors that are pertinent to this

level of reasoning. In the next section, we propose a micro-activity model for the skill-, rule-, and knowledge-based reasoning, which may be applied to the study performance. The models are used to show that the differences in workload between treatments may be explained by the rule-based reasoning that is needed to monitor the motion sickness during indirect vision in a moving vehicle. Further, the models are used to determine the relations among the ratings for the different measures and particularly, the relation of the perceived workload index to the ratings of task allocation of attention.

6. Micro-Activity Time Line Model

In this section of the report, we describe micro-activity time line models for direct and indirect vision targeting. In keeping with the literature, human response is assumed to be directed by micro-level activities that occur within cortical based processors, which consist of perceptual processors, a cognitive processor interfacing with memory, and a motor processor (Card, Morgan, & Newell, 1983). The processing times are assumed to be on the order of 100 milliseconds (Card, Morgan, & Newell, 1983), with a demand loading corresponding to the attention needed to process the information for the task (McCracken & Aldrich, 1984). Furthermore, loading is assumed to be increased by interference that occurs within processors during the performance of concurrent tasks (Little et al., 1993).

Here, skilled reasoning is interpreted as a sequence of over-learned, automatic activities performed in a pipelined manner between connected processors, from perceptual to cognitive and then to motor action. In contrast, rule-based reasoning is interpreted as being a cognitive processor activity of an evaluation nature, particularly of an "if-then" production rule. Finally, knowledge-based reasoning is interpreted as a cognitive activity involving memory recall and processing. The development of the models is guided by the results of the workload analysis, that is, knowledge-based reasoning remains consistent across treatments, while aspects of the skill- and rule-based reasoning are changed by the indirect vision. Further, the activities are restricted to the experimentally derived task times for the treatments. We describe first the model for stationary, direct vision without sound localization and then the model for indirect vision with the HMD in the moving vehicle with sound localization. These two treatments are extreme cases for the reported perceived workload.

6.1 Case I: Direct Vision, Stationary Vehicle, Without Sound Localization

Table 11 is a chart of a micro-activity time line for Case I. The trial status is listed in the "mode" column as a function of the trial times listed in the "time" column in milliseconds. The actions of the experimenter and the range control operator are listed in the "tester" and "range" columns, respectively. The micro-activities performed by the participant are listed in an activity column,

Table 11. Micro-Activity Time Line Chart for Case I: Direct Vision, Stationary Vehicle, Without Sound Localization

Mode	Time	Tester	Range	Participant	Base	Audio	Visual	Cognitive	Motor	Memory	Interval	Loading Anchor	Workload
Start run	0	flag up											
Detection	170		c/c key										
	960	command	target up										
	1060			listening	R	X					100	4.9 interpret speech	0.49
	1060			eyes open	R				X		70	2.2 discrete activation	0.154
search	1130			check	R			X			[70]	3.7 sign recognition	0.259
	1230			glimpse	S		X				100	3.7 discriminate	0.37
	1230			index eyes	S				X		100	2.2 discrete activation	0.22
	1230			check	S			X			[70]	3.3 alternative	0.231
repeat x6	1330			search	S		X						4.926
	2530			glimpse	S		X				100	3.7 discriminate	0.37
	2630			decision	R			X			70	4.6 judgement (single aspect)	0.322
	2700			switch mode	K			X		X	1350	5.3 recall	7.155
	2700	respond		vocal	R				X		[1000]	1 speech	1
	2700			vocal	R			X			[1000]	5.45 interference	5.45
	2870	move flag											
	3370	flag up											
Identification	3540		c/c key										
	4050			move	R				X		360	2.6 continuous adjustment	0.936
	4050			move	R				X		360	2.6 continuous adjustment	0.936
	4410			glimpse	R		X				100	5 inspect	0.5
	4510			index head	R		X		X		200	5.8 adjustive	1.16
	4710			glimpse	S		X				100	4 inspect	0.4
	4710			hand	R				X		[70]	2.1 discrete activation	0.147
	4710			check	S			X			[70]	3.7 sign recognition	0.259
zoom	4810			glimpse	S		X				[100]	4 inspect	0.4
	4810			index head	S		X		X		[100]	2 discrete activation	0.2
	4810			hand	S				X		[70]	2 discrete activation	0.14
	4810			check	S			X			[70]	3.7 sign recognition	0.259
repeat x19	4910			zoom	R		X				100	4 inspect	18.981
	6810			glimpse	R		X				100	4 inspect	0.4
	6910			decision	R			X			150	6.8 judgement (4+1 aspects)	1.02
	7060	respond		switch mode	K			X		X	1350	5.3 recall	7.155
	7060			vocal	R				X		[1000]	1 speech	1
	7060			vocal	R			X			[1000]	6.55 interference	6.55
	7230	move flag											
	7730	flag up											
End run	7900		c/c key										
End recall	8410												

Total workload = 60.464

Note: [**] bracketed times concurrent

with the type of reasoning that the activity uses indicated in the "base" column with the letter "K" for knowledge-based, "R" for rules-based, and "S" for skill-based reasoning. The cortical processors involved in these activities are listed in the next set of columns. The time to perform each activity is listed in the interval column, followed by the attention loading and the equivalent verbal anchor. Finally, the workload incurred is listed as the product of attention loading × the processor time interval.

According to the experimental results for Case I, the time to detect the target averaged 3.367 seconds and that to identify the orientation of the Landolt C-ring attached to the face of the target was 4.390 seconds (Smyth, 2002b). These times are measured from the facility control key actions, and the trial times listed in the table are adjusted for time used by the experimenter to start the trial. As noted in the activity columns, the participant at the start is waiting for the verbal command from the experimenter ("tester") to begin searching for the target. The command is given about 1 second after the experimenter has raised the signal flag. This allows enough time for the facility control operator to respond by activating the computer control key (170 milliseconds [ms] for visual perception and motor response) and for the target board to be completely raised by the mechanism (about 0.75 second).

Upon hearing the command to start the detection process, the participant opens his eyes and cognitively confirms the audio input. This is interpreted as a rule-based behavior with the cognitive action occurring concurrently with the oculomotor action. The participant then executes a sequence of skill-based activities consisting of a visual glimpse followed by the indexing of the eyes and head across the visual scene. Since the eye movements are saccadic, visual perception can only occur during the consequent fixation period. Concurrent with the motor action is a cognitive confirmation of the target absence. The cognitive activity is assumed to be pipelined with the previous visual perception. Finally, in this process, the participant realizes that he has seen the target and activates a verbal response. This last behavior is interpreted as rule based. Following a 170-ms delay for audio perception and motor response, the experimenter takes 500 ms to raise the signal flag to indicate detection. In turn, after another 170-ms delay (visual perception and motor response), facility control has activated the computer control key, thereby recording the detection event and the start of the identification process.

Concurrent with verbal delivery, the participant recalls from memory his knowledge of the procedure for the identification task. Since he is switching his procedural mode, we estimate that the time for recalling and establishing the procedural rules and cognitive reference frame is about 1.35 seconds as reported in the literature (Card, Moran, & Newell, 1980). Associated with the recall is an increase in attention loading because of interference between cognition and speech delivery (Little et al., 1993). In this model, the interference is further aggravated by previous priming of the cognitive working memory for judgment of the target sighting. The increase in loading is expressed as the sum of the separate task loadings x a conflict factor, which is commonly 0.5 for interference between the cognitive processor and the motor processor for speech (Allender, 1998).

Following setup, the participant moves the binoculars to his eyes and indexes his head in a rule-based activity to center the target within the visual field. The participant then proceeds to "zoom in" on the target in a skill-based sequence of visual glimpses. These glimpses are accompanied with concurrent hand adjustments for scene magnification, eye and head adjustments for centering the visual field, and a cognitive check of the scene. In this case, the eyes are fixed on the target, and the eye movements track the target as movements are induced in the scene by the increased magnification. These concurrent activities are automatically pipelined to the previous visual perception. Finally, the participant, realizing that he has seen the Landolt ring on the target, reports the orientation as "ID up," "ID down," "ID left," or "ID right". This last is interpreted as a rule-based behavior. Again, concurrent with his verbal delivery, the participant recalls from memory his knowledge of the procedure for actions between trial runs, that is, to turn his head down range and close his eyes. As before, associated with the recall is an increase in attention loading because of interference between cognition and speech delivery. Again, the interference is further aggravated by previous priming of the cognitive working memory for judgment of the target identification. Following a 170-ms delay for audio perception and motor response, the experimenter again takes 500 ms to raise the signal flag to indicate identification. In turn, after another 170-ms delay (visual perception and motor response), facility control has activated the computer control key to record the identification event and the end of the trial.

The amount of mental workload incurred in performing the activity is indicated in the last column. The workload increment for the processor is the product of the attention loading × the processor interval expressed in seconds. The total workload incurred in target detection and identification is the sum of the workload increments. For stationary direct vision without sound localization, the total workload incurred is 60.464 in units of attention loading × seconds, modeled over a 7.450-second time line including the final procedural recall for the trial run.

6.2   Case II: Indirect Vision With HMD, Moving Vehicle, With Sound Localization

Table 12 is a chart of a micro-activity time line for Case II. The chart has the same format as Table 11 for direct vision, with additional activities for the primary task of target search that are associated with the sound localization and facility mapping during vehicle movement. While the initial response to the sound tone is a rule-based head shift to the localizing direction, the participant ignores the tone during the rest of the trial and processes the audio perception at a skill-based orientation loading level. This is because following initial localization, the participants preferred to continue the search with the finer resolution of the visual process. This result is apparent in the data reported in other studies with target detection via an HMD with sound localization (Nelson et al., 1998). Note the interference between the motor processor during the head-turning response for initial localization and the audio processing of the tone. As before, the increase in loading is expressed as the sum of the separate task loadings × a 0.5 conflict factor.

Table 12. Micro-Activity Time Line Chart for Case II: HMD, Moving Vehicle, With Sound Localization

Mode	Time	Tester	Range	Participant	Task	Base	Somatic	Audio	Visual	Cognitive	Motor	Memory	Interval	Loading Anchor	Workload
Start run	0	flag up													
Detection	170		c/c key												
	960	command	target up	listening	1	R		X					100	4.9 interpret speech	0.49
	1060			eyes open	1	R					X		70	2.2 discrete activation	0.154
	1060			check cmd	1	R				X			[70]	3.7 sign recognition	0.259
	1130	tone		localize	1	R		X					100	4.2 selective orientation	0.42
	1230			index head	1	R					X		200	5.8 discrete adjustment	1.16
	1230			localize	1	S		X					[100]	3.3 orient	0.33
	1230				1	R		X			X		[100]	4.55 interference	0.455
	1230			check audio	1	R				X			[70]	3.7 sign recognition	0.259
search	1430														
look	1430			glimpse	1	S			X				100	3.7 discriminate	0.37
	1430			compute fix	1	R				X			[70]'	6.8 evaluation	0.476
	1430			fix view	1	R					X		[70]"	5.8 discrete adjustive	0.406
	1430			motion	2	S	X						[100]	4.2 selective orientation	0.42
	1430			shift head	2	S	X				X		[70]'	2.6 continuous adjust	0.182
	1430			conflicts	1	R			X	X	XX		[70]	13.23 interference	0.9261
	1530			check scene	1	S				X			70	3.7 recognition	0.259
	1600			remap	1	S				X		X	70	3.7 recognize	0.259
	1630	tone		localize	1	S		X					[200]	3.3 orient	0.66
	1630			conflict	1	R		X		X	X		[200]	6.274 interference	1.2598
	1670			index eyes	1	S					X		100	3.8 adjustment	0.38
	1670			conflict	2	S					XX		[100]	4.48 interference	0.448
	1770			resolve	2	R				X			70	4.6 evaluation	0.322
	1770			conflict	2	R				XX			[70]	5.81 interference	0.4067
	1770			conflict	2	R			X	X			[70]	4.15 interference	0.291
	1840			look	1	S			X						
repeat x6	4300			glimpse	1	S			X				100	3.7 discriminate	0.37
	4300			compute fix	1	R				X			[70]'	6.8 evaluation	0.476
	4300			fix view	1	R					X		[70]"	5.8 discrete adjustive	0.406
	4300			motion	2	S	X						[100]	4.2 selective attention	0.42
	4300			shift head	2	S	X				X		[70]'	2.6 continuous adjust	0.182
	4300			conflicts	1	R			X	X	XX		[70]	13.23 interference	0.9261
	4300			check scene	1	S				X			70	3.7 recognition	0.259
	4400			remap	1	S				X		X	70	3.7 recognition	0.259
	4470			compare	1	R				X			70	4.6 judgement (single)	0.322
	4540			index head	1	S					X		100	3.8 adjustment	0.38
	4610			conflict	2	S					XX		[100]	4.48 interference	0.448
	4610			resolve	2	R				X			70	4.6 evaluation	0.322
	4710			conflict	2	R				XX			[70]	6.44 interference	0.4508
	4710			conflict	2	R			X	X			[70]	4.15 interference	0.291

	Time	Event	Process	Code							Bracket	Description	Value
repeat x1	4780		search										
	8130	tone	localize	1 S	X			X			[200]	3.3 orient	0.66
	8130		conflict	1 R	X			X			[200]	15.098 interference	3.02
	8140		glimpse	1 S		X			X		100	4 inspect	0.4
	8140		compute fix	1 R			X	X			[70]'	6.8 evaluation	0.476
	8140		fix view	1 R						X	[70]''	5.8 discrete adjustive	0.406
	8140		motion	2 S		X	X	X			[100]	4.2 selective attention	0.42
	8140		shift head	2 S		X	X	X			[70]'	2.6 continuous adjust	0.182
	8140		conflicts	1 R			X	XX			[70]	13.38 interference	0.9366
	8240		decision	1 R			XX	XX				4.6 judgement (single)	0.322
	8310		resolve	2 R		X	X	X			70	4.6 evaluation	0.322
	8310		conflict	2 R			X	X			70	6.44 interference	0.4508
	8310		conflict	2 R							[70]	4.3 interference	0.301
	8380		switch mode	1 K						X	[70]	5.3 recall, shift mode	7.155
	8380	respond	vocal	1 R		X	X	X			[1000]	1 speech	1
	8380		conflict	1 R		X		X			[1000]	10.82 interference	10.82
	8550	move flag											
	8630	tone	localize	1 S	X		X	X			[200]	3 orient	0.6
	8630		conflict	1 R	X		X	X			[200]	10.06 interference	2.012
	9050	flag up											
	9130	tone	localize	1 S	X		X	X			[200]	3 orient	0.6
	9130		conflict	1 R	X		X	X			[200]	10.06 interference	2.012
Identification	9220	c/c key											
	9630	tone	localize	1 S	X		X	X			[200]	3 orient	0.6
	9630		conflict	1 R	X		X	X			[200]	8.1 interference	1.62
	9730		move	1 R						X	360	2.6 continuous adjust	0.936
	10090		glimpse	1 R		X					100	5 locate	0.5
	10090		compute fix	1 R			X	X			[70]'	6.8 evaluation	0.476
	10090		fix view	1 R				X			[70]''	5.8 discrete adjustive	0.406
	10090		motion	2 S	X						[100]	4.2 selective attention	0.42
	10090		shift head	2 S	X						[70]'	2.6 continuous adjust	0.182
	10090		conflicts	1 R		X	X	X			[70]	13.88 interference	0.9716
	10130	tone	localize	1 S	X		X	X			[200]	3 orient	0.6
	10130		conflict	1 R	X		X	X			[200]	7.704 interference	1.5408
	10190		remap	1 R				X		X	70	3.7 recognition	0.259
	10260		index head	1 R			X	X			200	5.8 discrete adjustive	1.16
	10260		conflict	2 R			XX	XX				5.88 interference	0.588
	10460		resolve	2 R		X	X				[100]	4.6 judgement (single)	0.322
	10460		conflict	2 R		X	XX				70	5.81 interference	0.4067
	10460		conflict	2 R		X	X				70	4.8 interference	0.336
	10530		glimpse	1 S								4 inspect	0.4
	10530		compute fix	1 R			X	X			[70]'	6.8 evaluation	0.476
	10530		fix view	1 R							[70]''	5.8 discrete adjustive	0.406
	10530		motion	2 S	X						[100]	4.2 selective attention	0.42

ID		Task	Res								Value	Description	Number
10530		shift head	2 S		X			X				2.6 continuous adjust	0.182
10530		conflicts	1 R				X	XX		[70]		13.38 interference	0.9366
10630	tone	localize	1 S		X					[200]		3 orient	0.6
10630		conflict	1 R		X		X	X		[200]		3.8225 interference	0.7645
10630		check scene	1 R						X		70	4.6 judgement (single)	0.322
10700		remap	1 S				X	X			70	3.7 recognize	0.259
10770		index head	1 R				X	XX			200	5.8 discrete adjustment	1.16
10970		hand	1 R								70	5.8 discrete adjustment	0.406
10970		conflict	2 R				X			[70]		8.12 interference	0.5684
11040		resolve	2 R				XX				70	4.6 judgement (single)	0.322
11040		conflict	2 R			X	X			[70]		5.81 interference	0.4067
11040		conflict	2 R			X				[70]		4.3 interference	0.301
11110		glimpse	1 S				X				100	4 inspect	0.4
11110		compute fix	1 R				X	X		[70]'		6.8 evaluation	0.476
11110		fix view	1 R							[70]"		5.8 discrete adjustive	0.406
11110		motion	2 S	X						[100]		4.2 selective attention	0.42
11110		shift head	2 S	X			X	XX		[70]'		2.6 continuous adjust	0.182
11110		conflicts	1 R				X	X		[70]		13.38 interference	0.9366
11130	tone	localize	1 S		X					[200]		3 orient	0.6
11130		conflict	1 R		X		X	X	X	[200]		6.558 interference	1.974
11210		remap	1 S								70	3.7 recognize	0.259
11280		index head	1 S								200	2.5 adjustment	0.5
11280		hand	1 S							[70]		2.5 adjustment	0.175
11280		conflict	2 S				X	X		[70]		3.5 interference	0.2499
11280		check scene	1 S				X	X		[70]		3.7 recognize	0.259
11480		resolve	2 R				XX	XX			70	4.6 judgement (single)	0.322
11480		conflict	2 R			X	X	X		[70]		5.81 interference	0.4067
11480		conflict	2 R							[70]		4.3 interference	0.301
11550		zoom												
15550		glimpse	1 R		X		X				100	4 inspect	0.4
15070		compute fix	1 R					X		[70]'		6.8 evaluation	0.476
15070		fix view	1 R							[70]"		5.8 discrete adjustive	0.406
15070		motion	2 S	X						[100]		4.2 selective attention	0.42
15070		shift head	2 S				X	X		[70]'		2.6 continuous adjust	0.182
15070		conflicts	1 R				X	XX	X	[70]		13.38 interference	0.9366
15130	tone	localize	1 S		X					[200]		3 orient	0.6
15130		conflict	1 R		X		X			[200]		6.406 interference	1.2813
15170		decision	1 R								150	6.8 judgement (4+1)	1.02
15320		resolve	2 R								70	4.6 judgement (single)	0.322
15320		conflict	2 R	X			X	X		[70]		7.98 interference	0.5586
15320		conflict	2 R				X	X		[70]		4.3 interference	0.301
15390		switch mode	1 K						X		1350	5.3 recall, shift mode	7.155
15390	respond	vocal	1 R				X	X		[1000]		1 speech	1
15390		conflict	1 R				X			[1000]		11.59 interference	11.59

15560 move flag							
15630 tone	localize	1 S	X		[200]	3 orient	0.6
15630	conflict	1 R	X	X	[200]	10.445 interference	2.089
16060 flag up							
16130 tone	localize	1 S	X		[200]	3 orient	0.6
16130	conflict	1 R	X	X	[200]	10.445 interference	2.089
End run 16230	c/c key						
16630 tone	localize	1 S	X		[200]	3 orient	0.33
16630	conflict	1 R	X	X	[200]	4.15 interference	o.4565
End recall 16740						Total workload = 245.114	

40

Vehicular movement increases the cognitive load on the participants. This is because the scene being searched is continually changing as the vehicle moves forward alongside the target facility. Consequently, in preparation for each ocular and head shift during target search, the participant cognitively rotates a mental map of the facility to find his next viewing point. Note that in preparation for the experiment, the participant was allowed to study the facility and target locations before the trials. This mental mapping process is repeated during zooming for target identification, since the movement of the vehicle tends to move the viewing point past the target. In shifting his view to compensate for the movement, the participant must again mentally maintain his location on the facility. During a visual glimpse, the participant concurrently holds and evaluates a head and eye orientation for effective acquisition; these activities are performed in a pipelined manner from the previous images. Following visual acquisition, the scene is evaluated for the presence of the target during detection or whether the target is centered during identification, with the latter performed concurrently with the head movement during the image zooming process.

Added to Table 12 are two columns for activities associated with the processing of motion sickness during vehicle movement as a second task. Associated with each eye glimpse is the generation of sensory conflict between the visual and sensorimotor activities, which involve the vestibular system through head movements. This sensory conflict is assumed to be perceived by a somatic processor, possibly with associated autonomic responses leading to pallor, drowsiness, salivation, sweating, nausea, and finally, vomiting in the more severe cases of sickness. Concurrent with the somatic perception is a head movement by a participant experienced with the indirect vision system, to counter the sensations through opposing movements of the vestibular system. However, the head movement response is based on the previous visual image, and the residual somatic sensation is evaluated in a following cognitive activity at the rules level.

As before, associated with the performance of concurrent tasks is an increase in attention loading because of interference within and between processors (Little et al., 1993). However, unlike the model for Case I, interference is a major source of processor loading. Essentially, we expect interference within the motor processor between head holding and control adjustment for the sighting task and head shifting to counter motion sickness. Further, we expect interference within the cognitive processor during sickness resolution because of the previous priming for scene mapping. Similarly, we expect interference between the visual and cognitive processors during resolution because of the previous associations for scene mapping. Finally, we expect interference between the visual and audio processors during sound localization cueing. The increase in loading is expressed as the sum of the separate task loadings × a conflict factor, which is commonly 0.7 for interference within a processor and 0.5 for interference between the visual and cognitive processors (Allender, 1998). The following is a more detailed description of the effect of interference on the loading of the processors.

Consider first the detection task, particularly the "look" portion of the search routine. As shown in Table 12, interference occurs within the motor processor during a visual glimpse because of

the conflict between the head and eye shift, which is needed to fix the view for the sighting task, and the concurrent head shift used to counter motion sickness. Similarly, interference occurs within the cognitive processor between the visual and somatic perceptions during scene mapping. Further, the previous priming of the motor processor for head adjustment interferes with indexing the eyes to the next scene fixation point. Similarly, the retention of the visual perception in working memory and the priming of the cognitive processor for computing the scene fixation interferes with resolution of the residual motion sickness. Finally, the audio perception of the tone interferes with the cognitive and motor processing, further aggravating the existing interference because of the suppression of the localizing response. A similar argument applies to the head adjustment portion of the search routine, except that here, the interference in the cognitive processor is caused by the previous priming for evaluation and judgment. This effect of previous evaluation applies also to interference in the cognitive processor during target verification following search and to interference from the audio tone. As with the model for Case I, there is interference between the speech for target detection and the cognitive recall of the identification task; here again, the previous priming for evaluation is expected to increase the cognitive load. The tones during speech further aggravate the existing cognitive interference.

Similar comments apply to the identification task. The visual glimpse has associated with it interference in the motor processor because of conflict with the body movements used in scene centering during zooming and the head shifts used to counter motion sickness. Again, interference occurs within the cognitive processor between the visual and somatic perceptions during scene mapping for maintaining the view on the target. Further, the previous priming of the motor processor for head adjustment to maintain the view interferes with the hand and fingers movements to increment magnification. The retention of the visual perception in working memory and the priming of the cognitive processor for computing the scene fixation interferes with resolution of the residual motion sickness. The audio perception of the tone interferes with the cognitive and motor processing, further aggravating the existing interference because of the suppression of the localizing response. This effect of previous evaluation applies also to interference in the cognitive processor during identity verification following zooming and to interference from the audio tone. There is interference between the speech for target identification and the cognitive recall of the trial preparation task; here again, the previous priming for evaluation is expected to increase the cognitive load. Also, the tones during speech further aggravate the existing cognitive interference.

Notice that the model proposed here for Case II follows the dictates of the data analysis of workload presented before. While the knowledge-based activities of recalling the identification procedure rules and reference frame remain consistent across models, the skill- and rule-based activities are changed. The increase in search time for the indirect vision is consumed by the response to motion sickness. However, the addition of the motion sickness response task has greatly increased the rule-based activities. Furthermore, the vehicle movement has increased the cognitive rule-based activities.

According to the experimental results for Case II, the time to detect the target averaged 9.054 seconds and time to identify the Landolt C-ring orientation was 7.010 seconds (Smyth, 2002b). These times are measured from the facility control key actions, and the trial times listed in the table are adjusted for the time taken by the experimenter to start the trial. The amount of mental workload incurred in performing the activity is indicated in the last column. The workload increment for the processor is the product of the attention loading $\times$ the processor interval expressed in seconds. The total workload incurred in the target detection and identification task is the sum of the workload increments. For this model, the total workload incurred is 245.114 in units of attention loading $\times$ seconds, modeled over a 15.43-second time line.

6.3   Relation to Mental Workload Measures

From the model structure, we determine the relations of the ratings for the micro-activity time line models to the mental workload measures of allocation of task attention, SA, motion sickness, and subjective stress.

6.3.1 Allocation of Task Attention

Table 7 shows that the loading ratings reported by the participants for the measures of the allocation of task visual and cognitive attention for the detection and identification tasks are statistically independent of the treatments. While this is also true for the psychomotor loading for the identification task, loading for the detection task depends on the vision treatment. Finally, the audio channel loading depends on the sound localization treatment for both tasks. In the SRK processing structure described before, the ratings of allocated attention dominate the SKILLS component. In Tables 11 and 12 for the micro-activity models, the skill activities are applied to the detection look and identification zoom portions of the time line. In particular, the sequence of a perceptual glimpse, cognitive verification, and motor indexing of the eyes and head is interpreted as a skill activity in both models. The average loading of the model for a channel performing a skilled activity is computed as the total incurred workload divided by the total time needed by the channel to perform the activity. For model verification, this loading may be compared to the rating scores reported for that channel by the participants in the experiment.

6.3.1.1 Detection Task

Here, we compare the attention loading of the channels for the model to that reported in the experiment for the detection task. We consider the results first for Case I and then for Case II. For the Case I model, the table shows that the model-derived loading of 3.700 for the visual channel is close to the average reported value of 3.575 and within the 95% confidence interval for the rating mean (4.122, 3.028). Similarly, the model-derived loading of 3.300 for the cognitive channel is close to the average reported value of 3.367 and within the 95% confidence interval (5.766, 2.968). In addition, the model derived loading of 2.200 for the psychomotor channel, is close to the average reported value of 1.788 and within the 95% confidence interval

(2.343, 1.233). Finally, the model-derived loading of 0.0 for the audio channel is close to the average reported value of 0.062 and within the 95% confidence interval (0.190, -0.066).

For the Case II model, the table shows that the model derived loading of 3.700 for the visual channel is close to the average reported value of 3.575 and within the 95% confidence interval for the rating mean (4.122, 3.028). Similarly, the model-derived loading of 3.700 for the cognitive channel is close to the average reported value of 3.367 and within the 95% confidence interval (3.767, 2.968). In addition, the model-derived loading of 3.800 for the psychomotor channel is close to the average reported value of 3.781 and within the 95% confidence interval (4.329, 3.233). Finally, model-derived loading of 3.300 for the audio channel is close to the average reported value of 3.293 and within the 95% confidence interval (3.861, 2.725). The results suggest that the ratings reported for the task-allocated attention agree with those used in the models and that the detection task is closely consistent across both models for the visual and cognitive channels.

6.3.1.2 Identification Task

We compare the attention loading of the channels for the model to that reported in the experiment for the identification task. We consider the results first for Case I and then for Case II. For the Case I model, the table shows that the model-derived loading of 4.000 for the visual channel is close to the average reported value of 3.973 and within the 95% confidence interval for the rating mean (4.462, 3.484). Similarly, the model-derived loading of 3.700 for the cognitive channel is close to the average reported value of 3.667 and within the 95% confidence interval (4.146, 3.188). In addition, the model-derived loading of 3.400 for the psychomotor channel (workload of 6.80 over 2.00 seconds) is close to the average reported value of 3.039 and within the 95% confidence interval (3.509, 2.569). Finally, the model-derived loading of 0.0 for the audio channel is equal to the average reported value.

For the Case II model, the table shows that the model-derived loading of 4.000 for the visual channel is close to the average reported value of 3.973 and within the 95% confidence interval for the rating mean (4.462, 3.484). Similarly, the model-derived loading of 3.700 for the cognitive channel is close to the average reported value of 3.667 and within the 95% confidence interval (4.146, 3.188). In addition, the model-derived loading of 3.375 for the psychomotor channel is close to the average reported value of 3.039 and within the 95% confidence interval (3.509, 2.569). Finally, model-derived loading of 3.000 for the audio channel is close to the average reported value of 2.725 and within the 95% confidence interval (3.332, 2118). The workload for the psychomotor channel is the sum of the skilled head and hand control adjustments. The results suggest that the ratings reported for the task-allocated attention agree with those used in the models and that the identification task is fairly consistent across both models for all but the audio channel.

6.3.2 Situational Awareness

Here, the objective of this study is to compare the ratings of the SART dimensions to those estimated from the micro-activity models, as determined from the loading of the model processors during rule-based activity. While the SART demand is expressed in cue properties, the micro-activity models presented do not support the resolution of the cue properties for analysis. However, the demand sum may be determined by the loading on the perceptual and cognitive processors of the model during rule-based encoding. In addition, the loading on the motor processor is included because of the effect on result assessment. In contrast, the micro-activity models presented do not support the analysis of the SART dimensions of attention resource capacity (i.e., supply) and the understanding of the situation. These dimensions depend on properties not included in the model. In particular, the cognitive properties, such as the state of alertness, the full cognitive capacity, concentration, and spread of attention focus, are not parameters in these models. The mental model determining the understanding is not part of the model either. For these reasons, only the SART demand sum is compared.

Referring to Table 11, the sum of the workload incurred for the rule- and knowledge-based processor activity of the Case I model is 33.698, which equates to an average loading of 8.596 over 3.92 seconds. Similarly, referring to Table 12, the workload incurred for the rule- and knowledge-based processor activity of the Case II model for the targeting task and motion sickness is 168.381, which equates to an average loading of 12.903 over 13.05 seconds. These results are listed in Table 13 for reference. For comparison to the SA ratings, the loading values need to be adjusted for the difference in the rating schemes. While the task-allocated attention is rated on a 0-to-7 scale (with verbal anchors), the SART dimensions are rated on a 1-to-7 scale. Considering that the SART demand is the sum of three dimensions and the model rule- and knowledge-based workload is summed over four processors, the scaling relation between the two rating schemes is $y = 0.643*x + 3$, assuming a linear relationship between the equivalent SART-demand (y) and the model loading (x).

Table 13. Comparison of SA Demand Sums

Treatments	SART demand statistics				Model			
	N	Sum mean	SD	Workload	Time (sec)	Loading	Demand	Ratio
Case I	32	8.225	4.279	33.698	3.92	8.596	8.527	0.96
Case II	32	11.538	4.614	168.381	13.05	12.903	11.294	1.02

With the scaling relation, the equivalent SART demand for the Case I model is 8.527; this value is within the 95% confidence interval (9.770, 6.680) for the average demand sum of 8.225 reported by the participants for experiment, according to the statistics listed in Table 6. Here, the ratio of the demand sum to the model demand is 0.96. Similarly, the equivalent SART demand

for the Case II model is 11.294, which is within the 95% confidence interval (13.204, 9.872) for the average demand sum of 11.538 reported by the participants. The ratio of the demand sum to the model demand is 1.02. These results suggest that the SART demand sum is measured by the equivalent demand for the model loading.

6.3.3 Motion Sickness

Motion sickness is interpreted as being caused by the sensory conflicts in the somatic perceptual processor and the associated cognitive assessment. An experienced gunner is assumed to naturally move his head in such a way as to induce movement of the vestibular system to counter conflicts with the visual scene. However, since the activity is pipelined, the motor activity is in response to a previous visual image instead of the most recent. The result is a skill-based sequence of somatic perception followed by a countering head shift that is generated with each visual glimpse. The conflict remaining is resolved by a rule-based cognitive activity. Since our model does not have the resolution to differentiate between symptom sources, we compare the model to the total severity of motion sickness. Furthermore, since the motion sickness reported was slight for the Case I model, the symptoms are ignored in the time line of Table 11. Considering the somatic perception, the associated head movement, and the resulting cognitive assessment, along with the associated interferences in Table 12 for the Case II model, the total severity loading is 7.669, since the incurred workload is 42.793 over the model time of 5.58 seconds. For comparison to the motion sickness ratings, the loading values need to be adjusted for the difference in the rating schemes. Although the task-allocated attention is rated on a 0-to-7 scale, each of the motion sickness dimensions is rated on a 0-to-3 scale. Although the model workload is summed over the three processors for a 0-to-21 scale, the total severity is a weighted sum of the 16 motion sickness dimensions resulting in a 0-to-120.54 scale (Kennedy, Lane, Lilienthal, Berbaum, & Hettinger, 1992). However, the severity distribution for the Case II treatments is heavily skewed toward lower values (skewness = 1.510, N = 16, standard error = 0.564), and weighting the scale by the ratio of the median (14.480) to the mean (22.199) results in a 0-to-78.62 scale. The scaling relation between the two rating schemes is $y = 3.744*x$, assuming a linear relationship between the equivalent total severity (y) and the model loading (x). With this relation, the equivalent total severity for the Case II model is 28.713, a value within the 95% confidence interval (34.634, 9.764) for the average total severity of 22.199 (N = 16, standard deviation = 23.342) reported by the participants.

6.4 Relation to Perceived Workload

We compare the workload incurred for the micro-activity time line models to the perceived workload reported by the experimental participants. We first compare the total perceived workload to the total workload incurred by the micro-activity models. We then compare the workload reported for each of the perceived dimensions. Essential to this work is the designation of sources within the model of the workload for the dimensions.

46

6.4.1 Total Workload

The NASA-TLX of mental workload is interpreted as the perceived task loading over the duration of the task. As described before, the total perceived TLX loading is the sum of the loadings for the measure dimensions. With this interpretation, the workload incurred is the product of the task loading and the course time. Referring to Table 11, the sum of the total workload incurred for the Case I model is 60.464, which equates to an average loading of 8.116 over the 7.45 seconds. Similarly, referring to Table 12, the total workload incurred for the Case II model is 245.114, which equates to an average loading of 15.886 over the 15.43 seconds. These results are listed in Table 14 for reference.

For comparison to the total TLX ratings, the loading values need to be adjusted for the difference in the rating schemes. Although the task-allocated attention is rated on a 0-to-7 scale, the TLX dimensions are rated on a 0-to-9 scale. Considering that the total TLX is the sum of six dimensions and the Case I model workload is summed over four processors, the scaling relation between the two rating schemes is $y = 1.928*x$, assuming a linear relationship between the equivalent total TLX-rating (y) and the model loading (x). With the scaling relation, the equivalent total TLX for the Case I model is 15.647; this value is within the 95% confidence interval (10.367, 17.298) for the average total TLX rating of 13.966 reported by the participants, according to the statistics in Table 6. Here, the ratio of the total TLX loading to the equivalent model loading is 0.90. Since the Case II model workload is summed over five processors, the scaling relation between the two rating schemes is $y = 1.543*x$. Consequently, the equivalent total TLX for the Case II model is 24.511, which is within the 95% confidence interval (32.075, 24.125) for the average sum of 28.100 reported by the participants. The ratio of the total TLX loading to the model equivalent is 1.14. These results suggest that the total TLX loading is measured by the equivalent model loading.

Table 14. Comparison of TLX Total Workload to Model Total Loading

| Treatments | TLX statistics | | | | | Model | | |
	N	Sum mean	SD	Workload	Time (sec)	Loading	Demand	Ratio
Case I	32	13.966	9.958	60.464	7.45	8.116	15.647	0.90
Case II	16	28.100	11.011	245.114	15.43	15.886	24.511	1.14

6.4.2 Workload Dimensions

We consider the relation of the workload dimensions to the micro-activity models. In particular, micro-processor configurations are mapped to the dimensions, and the resulting micro-activity loading values are compared to the rating statistics when possible.

6.4.2.1 Mental Demand

The dimension rates the amount of mental and perceptual activity that is needed to perform the task. We interpret mental demand as the amount of perceptual and cognitive activity used at the skill and rule levels but not knowledge recall, which is separate from the somatic response. Referring to Table 11, the sum of the workload incurred for the Case I model is 33.897, which equates to an average loading of 5.575 over 6.08 seconds. Similarly, referring to Table 12, the workload incurred for the Case II model is 148.292, which equates to an average loading of 12.493 over 11.87 seconds. For comparison to the TLX mental demand ratings, the loading values need to be adjusted for the difference in the rating schemes. Although the task-allocated attention is rated on a 0-to-7 scale, the TLX dimension is rated on a 0-to-9 scale. Since the Case I model workload is summed over three processors (audio, visual, and cognitive), the scaling relation between the two rating schemes is $y = 0.4286*x$, assuming a linear relationship between the mental demand rating (y) and the model loading (x). With the scaling relation, the equivalent mental demand is 2.389 for Case I. This value is within the 95% confidence interval (3.309, 1.503) for the average mental demand rating of 2.406 reported by the participants (N = 32, standard deviation = 2.503) for the direct vision treatments. Similarly, the Case II model is summed over the same three processors, and the equivalent mental demand is 5.354 for the Case II model, which is within the 95% confidence interval (5.569, 3.612) for the average mental demand rating of 4.591 reported by the participants (N = 32, standard deviation = 2.710) for the indirect vision treatments with the HMD.

6.4.2.2 Physical Demand

The dimension rates the amount of physical activity required to perform the task. We interpret physical demand as the amount of perceptual and motor skill-based activity used, which is separate from the somatic response. Referring to Table 11, the sum of the workload incurred for the Case I model is 19.700, which equates to an average loading of 5.472 over 3.60 seconds. With the scaling relation for the three-processor configuration (audio, visual, and motor), the equivalent physical demand is 2.345 for Case I. This value is outside the 95% confidence interval (1.745, 0.698) for the average physical demand rating of 1.222 reported by the participants (N=32, standard deviation = 1.450) for the direct vision treatments. Similarly, referring to Table 12, the workload incurred for the Case II model is 49.076, which equates to an average loading of 4.461 over 11.00 seconds. Considering that the model workload is summed over four processors, the scaling relation between the two rating schemes is $y = 0.3214*x$, assuming a linear relationship between the physical demand rating (y) and the model loading (x). Similarly, the equivalent physical demand is 1.434 for the Case II model, which is close to the 95% confidence interval (3.416, 1.708) for the average physical demand rating of 2.562 reported by the participants (N = 32, standard deviation = 2.366) for the indirect vision treatments with the HMD.

6.4.2.3 Temporal Demand

The dimension rates the pace at which the task was performed. We interpret temporal demand as the amount of perceptual activity for both the task and the somatic response. Referring to Table 11, the sum of the workload incurred for the Case I model is 12.750, which equates to an average loading of 3.984 over 3.20 seconds. With the scaling relation for two processors (audio and visual), given by $y = 0.6428*x$, the equivalent temporal demand is 2.561, which is within the 95% confidence interval (4.157, 2.212) for the average temporal demand rating of 3.184 reported for that treatment (N=32, standard deviation = 2.694). Similarly, referring to Table 12, the workload incurred for the Case II model is 118.888, which equates to an average loading of 14.769 over 8.05 seconds. Again, using a scaling relation of 0.4285 for three processors, the equivalent temporal demand is 6.328, which is near the 95% confidence interval (5.696, 3.835) for the average temporal demand rating of 4.766 reported for that treatment (N = 32, standard deviation = 2.577).

Analyses are not made for the TLX interaction dimensions of effort, performance, and frustration, since the micro-activity models do not include appropriate mental modeling as components. The rating of the effort dimension depends on previous experience with the tasks. A participant with more experience requires less effort to perform the same task. The performance dimension rates the success of the participant in accomplishing the task goals. The frustration dimension rates the satisfaction with performance. The evaluation of these dimensions requires inclusion of mental models of experience, goals, and motivation, which are not part of the micro-activity models developed here. In the next section, the results of the mental workload analysis are incorporated into a task analysis workload simulation of the targeting task. The results are that the task workload is expanded to include additional components of perceived workload in the simulation through the effects of SA and motion sickness.

7. Mental Workload Simulation

Following the micro-activity models described before, the mental workload is incorporated into a task analysis workload simulation. In this development, workload is defined as the amount of effort, both physical and psychological, that is expended in response to system demands according to an internal standard of performance (Stein, 1993). Here, target detection and identification are self-paced tasks and the task load is the time of execution and the error rate incurred according to the standards established during training (Smyth, 2002b). In this report, the task load is described in the section about task performance, while the mental workload is described in the sections about mental workload measures and micro-activity time line.

7.1 Simulation Modeling Program

The Improved Performance Research Integration Tool (IMPRINT) simulation modeling program (Allender, 1998), which is used to model the workload of the targeting task, was developed for ARL by Micro-Analysis & Design, Inc. The program consists of a set of Windows-based automated aids to assist analysts in conducting human performance analyses. In addition to being useful for estimating crew workload, IMPRINT provides the means for estimating manpower, personnel, and training requirements and constraints for new weapon systems early in the acquisition process.

An essential step in the workload analysis is defining the system mission and the functions and tasks to be performed by the crew in that mission. A hierarchy of task analysis network diagrams is used to depict the functions and the tasks. The network links together the tasks in a sequence of activities with the tasks denoted by the network branches and task completion by the nodes. Depending on the result of a task activity, branching to the next task can occur among tasks connected to the same node. This branching is dictated by a set of branching rules, which may be probabilistic, repeating, or tactical in form. Associated with each task are the specifications for the statistics of the performance time, the accuracy of the result, and the effects on the branching rules. In an advanced version, the task may be subdivided into micro-state activities with associated component times. Also associated with each task are attention loading values for activation of the human visual, auditory, cognitive, and psychomotor information processing channels during task performance and the additional loading attributable to channel conflicts. The attention loading values may be combined into an overall workload measure. Workload management strategies may be designated to handle work overload. The machine displays and controls with which the crew member interfaces are assigned channels as resources that are activated for operations. In turn, the interfaces are assigned to the tasks. Finally, the individual crew members are assigned tasks.

When the simulation model is executed, the tasks are scheduled and performed as specified in the flow diagrams and branching logic. As the tasks are performed, the total instantaneous workload prediction is calculated as the weighted sum of the load on each of the channels at a moment in time as rated with the loading values and a factor that accounts for the amount of conflict between and within resources that are used in parallel. The predicted workload output is a measure of the amount of effort that the tasks, the scenario, and the interfaces are imposing on the simulated operator.

This is, of course, a limited presentation of the full capabilities of the simulation program as it applies to workload for the extremely simplistic task of targeting. This is especially true when compared to the full range of successful application to simulating in-depth operations and maintaining a wide range of military vehicles and helicopters. However, the construction of a simulation model allows us to consider perceived workload as an addition to the task workload,

particularly the effects of SA and motion sickness that result from our field study and consequential analysis.

7.2 Simulation Model

Next, we construct a simulation model for the targeting task. We consider the task network diagrams, the resource interface assignments, channel loading values, task activity times, and branching decision rules, and we discuss a representative simulation output.

7.2.1 Task Network Diagrams

Figure 6 is a function-level network flow diagram for the IMPRINT representation of the task. The figure shows an experimental trial consisting of a trial start, target detection, identification, correct identification, and trial end. The figure includes IMPRINT decision nodes for the probabilities of detection, identification, and correct identification. The tasks for the detection and identification stages are further described in the following network flow diagrams.
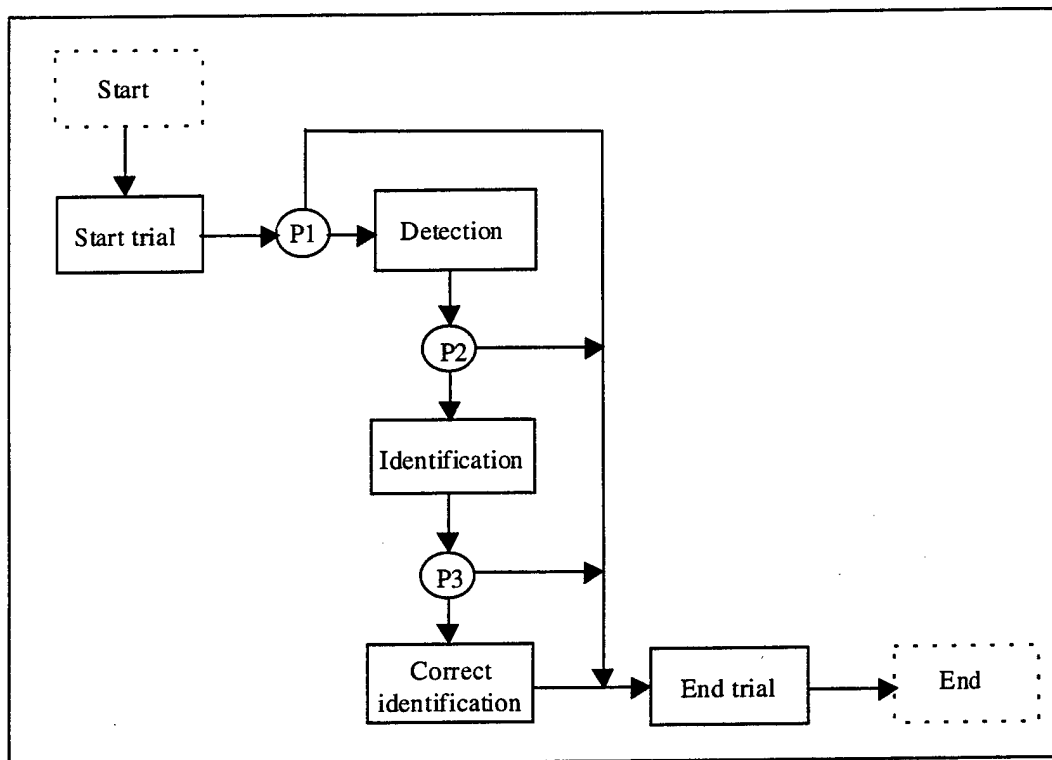
Figure 6. Functional Flow Diagram.

7.2.1.1 Detection Task

Figure 7 is an IMPRINT task level flow diagram for the detection task. Following the section about task analysis (see Figure 1), the diagram shows the task modeled as a closed loop sequence of visual glimpses executed with eye and head shifts for indexing the visual lobe. Vehicular motion causes the participant to re-center the view for each glimpse. The sequencing among the

loop branches is determined by IMPRINT decision rules. Here, the decision rule for the node T1 determines the number of times that the vision system must be indexed to view the target. For the return loop, the figure shows two path segments, one for indexing the eyes and the other for indexing the head when the vision is obscured by the viewing FOV, as determined by the decision rule for node T2. Once the visual lobe is directed to the target location, the decision rule for node T1 passes the simulation to the voice response and the task end node. Since in practice, an IMPRINT task flow is commonly diagrammed in terms of observable measures, these activities may be summarized as target search, and the detection task diagrammed as command response, search, and verbal response following detection.

7.2.1.2 Identification Task

Figure 8 is an IMPRINT task flow diagram for the identification task. Following the task analysis (see Figure 2), the diagram shows the task as a closed loop sequence of zoom (or magnification) adjustments in the viewing power, followed by a visual glimpse at the target. Zoom adjustment and vehicular motion cause the participant to re-center the view for each glimpse. The IMPRINT decision rule for the node T3 determines the number of times that the adjustments must be made to reach the proper magnification to identify the marker on the target. Once the adjustments are completed, the decision rule passes the identification to the voice response and the task end node. Again, these activities may be summarized as zooming, and the identification task may be diagrammed as control placement, zoom, and verbal response following identification.
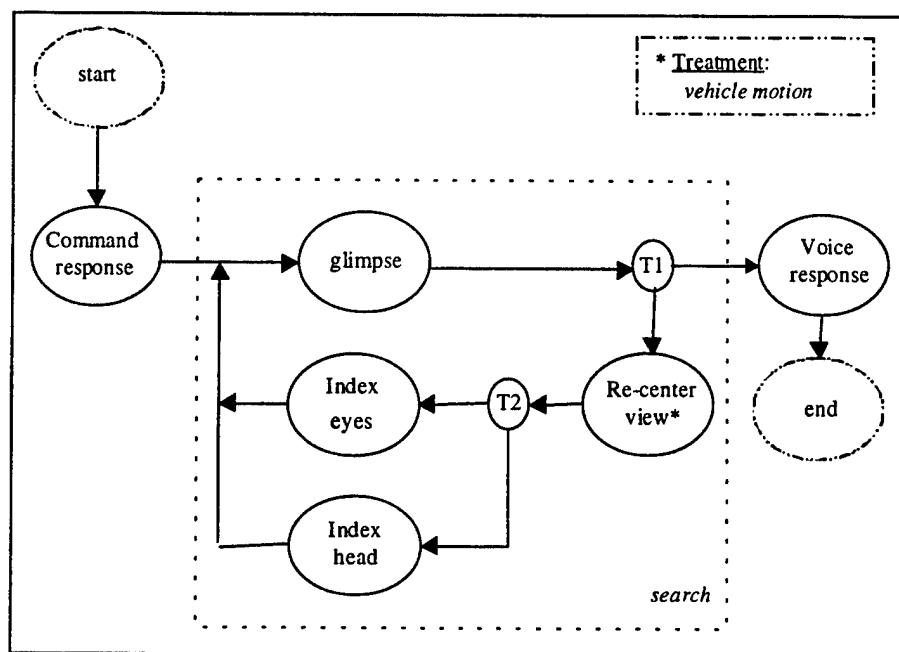

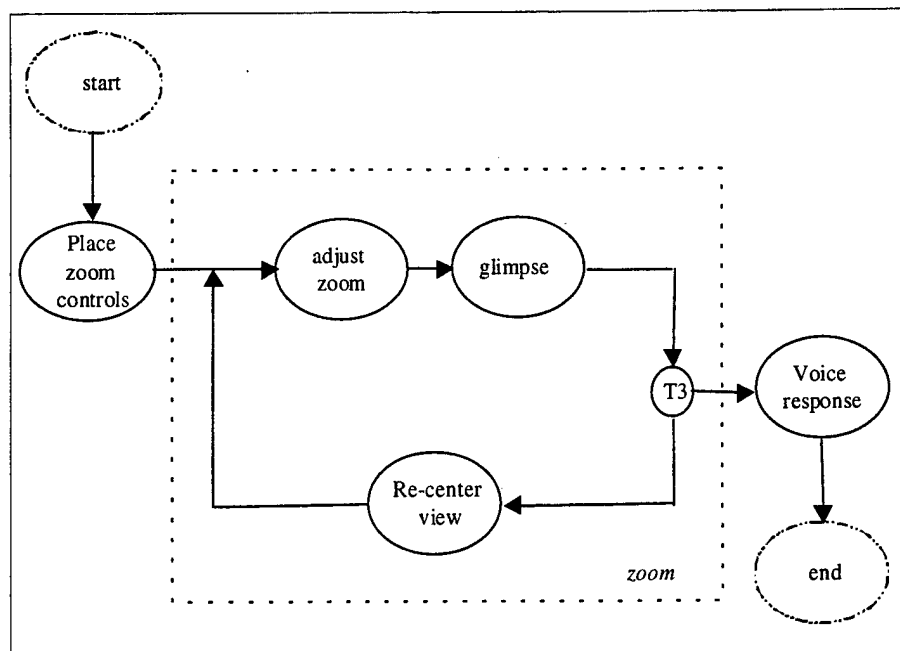Figure 7. Task-Level Flow Diagram for Detection.

Figure 8. Task-Level Flow Diagram for Identification.

7.2.2 Resource Interface Channels

Table 15 lists the resources and interfaces for the IMPRINT task model. As can be seen from the table, the interfaces between the participant and vehicle are the visual display, the auditory display, and the manual controls. The attentional resources of the participant include the visual, auditory, cognitive, and motor processors. The speech interaction with the experimenter is not included in the analysis.

Table 15. Workload Attention Resources and Interface Channels

Resources	Interfaces
Visual	Visual display
Auditory	Earphones
Cognitive	Visual display
Motor	Manual controls

Table 16 shows the relations between the interfaces and resources, that is, which interfaces place demands upon the attentional resources in the IMPRINT model. The table is a simple mapping of the input from the vehicle displays to the visual, audio, and cognitive channels, with the manual controls as the output of the motor channel.

53

Table 16. Relation of Operator Interface Channels to Attention Resources

Interface	visual	Attention Resources auditory	cognitive	motor
Visual Display	x		x	
Earphones		x		
Manual controls				x

7.2.3 Channel Loading Values

Tables 17 and 18 list workload demands placed by the tasks upon the resources via the interface channels in the IMPRINT model, for the two treatments of Case I: direct vision, stationary, without sound localization, and Case II: HMD, moving vehicle, with sound localization, respectively. In the tables, the loading values for the tasks are predicted from the micro-activity models of Tables 11 and 12. In this process, the loading for the task is calculated as the ratio of incurred workload during the task to the time that the loading occurred. In addition to listing the skill-based task allocation and rule-based SA demand for the tasks, the tables list the motion sickness severity. The total perceived work loading is also listed. In the micro-modeling section, it was demonstrated that the experimental measures agreed with the loading values derived from appropriate processor configurations for the micro-model time lines following dimension scaling. In this manner, the measures are scaled to the 7-point (0 to 7) loading factors scale (McCracken & Aldrich, 1984), used for allocated attention in the IMPRINT simulation modeling.

Table 17. Average Attention Loading Values for Case I: Direct Vision, Stationary, Without Sound

Task	Visual	Task Allocation Cognitive	Audio	Motor	Total	Awareness Demand	Motion Sickness	Total Workload
(a) Detection-								
Command	0.00	0.00	0.00	0.00	0.00	5.31	0.00	5.31
Search	3.70	3.30	0.00	2.20	8.21	0.00	0.00	8.21
Voice Response	3.70	0.00	0.00	0.00	3.70	8.19	0.00	7.89
(b) Identification-								
Place Controls	4.00	3.70	0.00	0.00	6.59	3.76	0.00	4.48
Zoom	4.00	3.70	0.00	4.00	9.99	0.00	0.00	9.99
Voice Response	0.00	0.00	0.00	0.00	0.00	7.95	0.00	7.95

Table 18. Average Attention Loading Values for Case II: Indirect Vision, Moving, With Sound Localization

Task	Visual	Task Allocation Cognitive	Audio	Motor	Total	Awareness Demand	Motion Sickness	Total Workload
(a) Detection-								
Command	0.00	0.00	3.30	0.00	3.30	6.80	0.00	7.50
Search	3.70	3.70	3.30	3.80	5.43	14.51	7.66	16.31
Voice Response	4.00	0.00	3.30	0.00	3.87	17.62	9.86	19.59
(b) Identification-								
Place Controls	4.00	3.70	3.00	0.00	3.75	11.18	8.82	12.87
Zoom	4.00	3.70	3.00	3.37	8.77	16.59	7.84	17.86
Voice Response	0.00	0.00	3.00	0.00	3.00	11.84	10.49	12.75

In each case, the table shows the loading applied over the full sub-task. These sub-tasks are the command response, search, and verbal response for detection, placement of controls, zoom, and verbal response for identification. This is true despite the fact that the activities of glimpse, index eyes, and re-center in the detection search task are sequential for both cases according to Tables 11 and 12. Further, the identification zoom glimpse activity is concurrent with the activities of the head and hand adjustments for Case I but sequential for Case II. In concept, the loading specifies the attention demand that is required to perform the mental function during the time that it is activated as part of the task. As demonstrated in the micro-activity models, a mental function is activated during part of the task and the loading only applies to that period and not to the entire task. However, we may compute the workload incurred as the loading applied over the task duration and summed over tasks; this approach results in workloads that are close in value via the model loading values or those that were experimentally collected. The implication is that we may consider the loading values as applying to the full sub-task duration. Note that in this simulation, the total loading is computed as a weighted sum of the loading values on the processors, in which the weights are the ratio of the duration of the processor activity to the behavior duration for the total loading as determined from the micro-activity model.

7.2.4 Task Activity Times

Table 19 lists the task activity times used in the simulation for the two treatment cases. The times are from the micro-activity models of Tables 11 and 12 with the processor activities blocked to match the task-level flow diagrams of Figures 7 and 8. The blocking used corresponds to the sub-tasks of command response, search, and verbal response for detection, placement of controls, zoom, and verbal response for identification.

Table 19. Task Activity Times (seconds)

| Task | Experimental Treatment | |
	Case I	Case II
(a) Detection-		
Command Response	0.17	0.47
Search	1.40	6.70
Voice Response	1.52	1.60
Total	3.09	8.77
(b) Identification-		
Place Controls	0.76	1.38
Zoom	2.00	3.96
Voice Response	1.25	1.32
Total	4.01	6.66
Grand Total	7.10	15.43

7.2.5 Branching Decision Rules

Table 20 lists the scenario variables used in the simulation; the status of the variables is used to control the branching logic of the task flow. Table 21 lists the IMPRINT branching logic for the probability nodes of Figure 6. Tables 22 and 23 list the decision rules for the looping nodes of Figure 7 for the detection task. Table 24 lists the rules for the looping node of Figure 8 for the identification task. The probabilities listed in Table 21 are derived from the experimental results. In the function diagram of Figure 6, the probability nodes control the branching of the task flow. The task times used to compute the logic of the decision nodes in Tables 22 through 24 are listed in Table 19. The task loop cycle times are computed from the sum of the times for the micro-activities needed to complete the loop cycle, as taken from Tables 11 and 12. These results agree with the times reported in the Micromodel library of IMPRINT (Allender, 1998; see also Little et al., 1993). The loop cycle is composed of a sequence of micro-level activities executed by the human to acquire and process information, make decisions, and execute actions. In the task diagrams of Figures 7 and 8, task choices are decided at looping nodes as a function of the state of the scenario variables.

7.3 Simulation Results

Figure 9 is a representative plot of the predicted mental loading produced by a simulation of the Case II treatment of HMD, moving vehicle, and sound localization. The plot shows the loading values from Table 18 for the total task allocation, SA demand, motion sickness severity, and perceived total workload, as a function of the task activities. The plot demonstrates that proper mapping of the elements of the simulation task flow network with the clusters of the mental workload measures can result in a reasonable simulation of the mental workload that occurs during the targeting tasks.

Table 20. Scenario Variables

Variable name	Type	Role
time_det	real	time to detect target from start of trial
time_id	real	time to identify target from time of detection
cycle_det	real	time period between indexing visual lobe
cycle_id	real	time period between indexing zoom control
tgt_ang	real	angular offset of target from initial search orientation
fov_device	real	FOV of viewing device
fov_glimpse	real	effective FOV of glimpse viewing lobe
max_vis	integer	total number of visual lobe shifts to reach target
index_vis	integer	index of visual lobe shifts
index_head	integer	index of number of head shifts for vision device
max_eyes	integer	total number of eye shifts to span vision device
index_eyes	integer	index of number of eye shifts for head position
max_zoom	integer	total number of manual zoom shifts
index_zoom	integer	index of manual zoom shifts

Table 21. Branching Logic for Probability Nodes of Trial Functional Flow Diagram in Figure 6

I. Probability Node, P1: Determine if successful target detection.
Case I treatment: Direct viewing, stationary, no sound localization

Following node	logic
Detection	P = 0.901;
End Trial	P = 0.099;

Case II Treatment: HMD, moving vehicle, sound localization-

Following node	logic
Detection	P = 0.307;
End Trial	P = 0.693;

II. Probability Node, P2: Determine if successful target identification.
Case I treatment: Direct viewing, stationary, no sound localization-

Following node	logic
Identification	P = 0.948;
End Trial	P = 0.052;

Case II Treatment: HMD, moving vehicle, sound localization-

Following node	logic
Identification	P = 0.305;
End Trial	P = 0.695;

III. Probability Node, P3: Determine if correct identification
Case I treatment: Direct viewing, stationary, no sound localization-

Following node	logic
Correctly Identified	P = 0.872;
End Trial	P = 0.128;

Case II Treatment: HMD, moving vehicle, sound localization-

Following node	logic
Correctly Identified	P = 0.611;
End Trial	P = 0.389;

Table 22. Branching Logic for Decision Node T1 of Detection Task Flow Diagram (see Figure 7)

Purpose: Determine when target detected
Method: Index visual lobe to target position.

(a) Initialize variables:

Task: Detection
Sub-task: Command Response

 Effect: Beginning

  Case I Treatment: direct vision, stationary, no sound cues

Variable name	value	units
time_det	1.400	seconds
cycle_det	200	millisecs

  Case II Treatment: HMD, moving, sound localization

Variable name	value	units
time_det	6.700	seconds
cycle_det	418	millisecs

 Effect: Ending

Algorithm: max_vis := time_det/cycle_det;

Variable name	value	units
index_vis	0	count

(b) Increment logic:

Task: Detection
Sub-task: Glimpse
 Effect: Ending

Algorithm: index_vis += 1;

(c) Branching logic:

Following node	logic
Recenter View	index_vis < max_vis;
Voice Response	index_vis >= max_vis;

Table 23. Branching Logic for Decision Node T2 of Detection Task (see Figure 7)

Purpose: Control head movement.
Method: Count number of eye shifts to reach head movement.

(a) Initialize variables

Task: Detection
Sub-task: Command Response

Effect: beginning

Case I Treatment: direct vision, stationary, no sound cues

Variable name	value	units
tgt_ang	30.0	degrees
fov_device	85.0	degrees

Case II Treatment: HMD, moving, sound localization

Variable name	value	units
tgt_ang	30.0	degrees
fov_device	13.125	degrees

Effect: Ending
Algorithm: fov_glimpse := tgt_ang/max_vis;
            max_eyes := fov_device/fov_glimpse;

Variable name	value	units
index_eyes	0	count
index_head	0	count

(b) Increment logic:

Task: Detection
Sub-task: Index Eyes
 Effect: Ending
Algorithm: index_eyes += 1;

Task: Detection
Sub-task: Index Head
 Effect: Ending
Algorithm: index_head += 1;
            index_eyes := 0;

(c) Branching logic:

Following node	logic
Index Eyes	index_eyes < max_eyes;
Index Head	index_eyes >= max_eyes;

Table 24. Branching Logic for Decision Node T3 of Identification Task Flow Diagram (see Figure 8)

Purpose: Control zoom movements.
Method: Count zoom indexes to see Landolt ring gap.

(a) Initialize variables:

Task: Identification
Sub-task: Place Zoom Controls

  Effect: beginning

  Case I Treatment: direct vision, stationary, no sound cues

Variable name	value	units
time_id	2.00	seconds
cycle_id	100	millisecs

  Case II Treatment: HMD, moving, sound localization

Variable name	value	units
time_id	3.96	seconds
cycle_id	440	millisecs .

  Effect: Ending

Algorithm: max_zoom := time_id/cycle_id;

Variable name	value	units
index_zoom	0	count

(b) Increment logic:

Task: Identification
Sub-task: Glimpse
  Effect: Ending
Algorithm: index_zoom += 1;

(c) Branching logic:

Following node	logic
Re-center View	index_zoom < max_zoom;
Voice Response	index_zoom >= max_zoom;
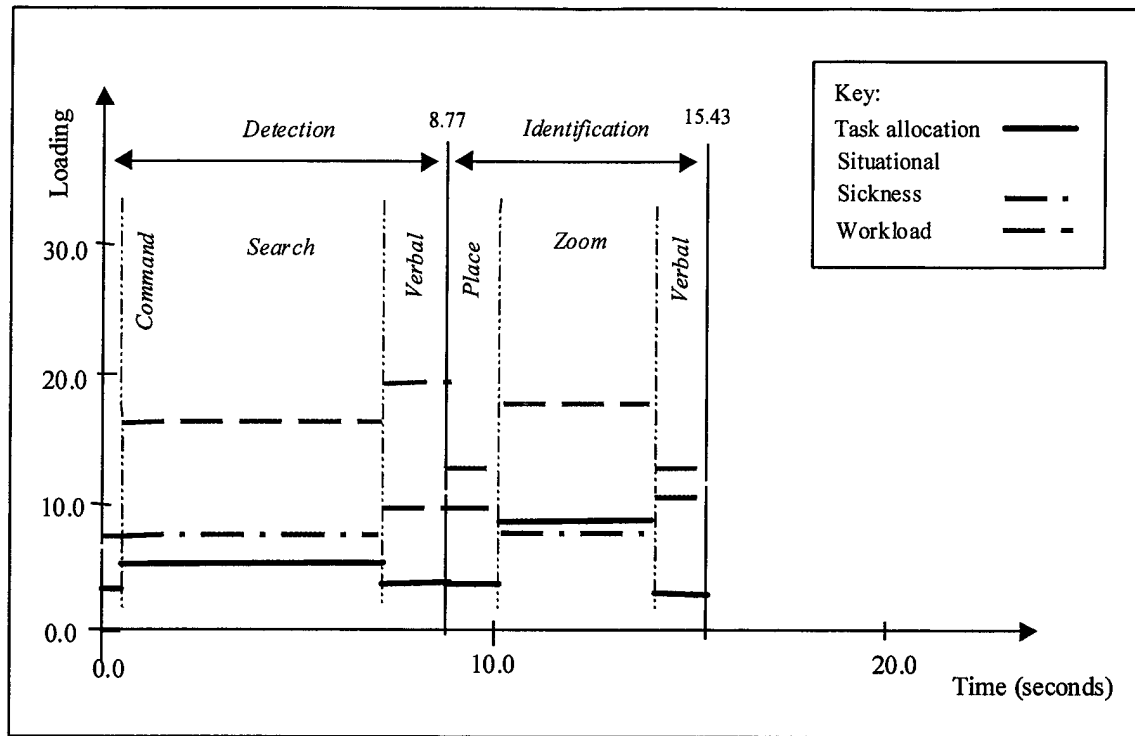
Figure 9. Simulation Output for Case II: HMD, Moving Vehicle, With Sound Localization.

7.4   Workload Cost Considerations

Human factors analysts may use the simulation of task workload to predict the effects on performance. In a two-person vehicle, the gunner may be expected to perform other functions such as navigation and communications. An increase in task workload, the demand on SA, and the chance of motion sickness may increase the psychological stress on the gunner. At high stress levels, the resulting physiological arousal is detrimental to performance. The immediate effect is to produce tunneling or narrowing of the perceptual and cognitive attention, in order to concentrate on the detection and identification tasks while ignoring the surroundings. There is a tendency toward working memory loss with reduced capacity for processing new or complex material and a focus on well-learned responses and a rapid execution of these responses at the expense of possible errors. The resultant shedding of secondary tasks may not be done in an optimal order for successfully coping with the problem environment. In particular, motion sickness distracts from the task since the discomfort is intrusive and the gunner cannot readily concentrate. Although the immediate task performance may degrade, the long-term effects are cumulative, resulting in accumulated fatigue over an extended period of time, which can adversely affect performance of subsequent tasks (Wickens, Gordon, & Liu, 1998).

8. Conclusion

The perceived workload for the targeting tasks is a function of the skill- and rule-based components of reasoning, which are formed from mental workload measures of task attention, SA, and motion sickness, at least for the data collected in our field experiment (Smyth, 2002b). A factorial analysis of the mental workload measures forms a cognitive component space that corresponds to an SRK model of information processing (Rasmussen, 1983). The measures tend to align with the components, depending on the level of reasoning. For example, the cluster for the task attention loading appears to be associated with a skill-based reasoning that is focused on the targeting tasks without much loading on the rule or knowledge components. In contrast, the motion sickness and SA demand measures are clustered along the rules component. Finally, the situation understanding measures are clustered along the knowledge component.

The mental workload measures are explained by a micro-state activity model of the targeting tasks that is based on an interpretation of human reasoning as the product of inter-linked perceptual, cognitive, and psychomotor processors (Card, Moran, & Newell, 1983). The model is expanded to include pipelined skilled behavior for task performance and body movement to compensate for motion sickness, as well as ruled-based behavior for the assessment of situation demand and motion sickness. Further, the model includes task switching and orienting responses to audio cues as intrusive stimuli. The development follows a generic information-processing model for which production rules are developed. The results of the cognitive component space analysis are used to further refine the model at the different levels of processing. It is argued that the mental workload measures correspond to different configurations of the model processors activated at the skill and rule-based level for the tasks of targeting and monitoring motion sickness. Of interest is that the loading values generated by the processor configurations significantly agree with the experimental values, following correction for the differences in scaling. Furthermore, significant matching of different configurations of the model processors occurs for the perceived workload and the demand dimensions. The results suggest a common micro-activity model source for these different facets of human behavior.

The loading values generated by the micro-state model are used in an expanded IMPRINT task analysis workload simulation modeling program for the inclusion of SA and motion sickness. In this process, the measures are scaled on the 7-point (0 to 7) loading factors scale (McCracken & Aldrich, 1984), used for allocated attention in the program. Note that in this simulation, the definitions of loading, workload, and total loading are tied to the micro-model activity as separate concepts. In particular, total loading is computed as a weighted sum of the loading values on the processors, in which the weights are the ratio of the duration of the processor activity to the behavior duration for the total loading, as determined from the micro-model. The

use of these concepts ensures definite relations between the simulation output and the experimental measures of SA and motion sickness, as well as perceived workload.

A remaining issue of research interest is the long-term effect of demand loading on crew performance. An increase in workload, demand on SA, or the chance of motion sickness may increase the psychological stress on the user of the indirect vision system. While the immediate task performance may be degraded, the long-term effects may be cumulative, resulting in accumulated fatigue over time, which can produce errors and adversely affect performance of subsequent tasks.

Finally, the task load performance and mental workload models derived in this report do not make explicit the higher cognitive processes that are used in targeting tasks. A review of the human information processing literature suggests cognitive mechanisms that are needed for a higher level model. The superposition of executive cognitive processes by an expert system, which consist of production rules, is needed to support the explicit declaration of rule-based reasoning. These higher cognitive processes are used to develop and apply the rule-based schematics that guide and direct the skill-based behavior. An essential element of this supervisory process is the development and maintenance of a mental model of the task and the battlefield situation.

9. Recommendations for Further Research

The author recommends that the micro-state model approach developed in this study be used in the analysis of performance and subjective evaluation data collected from experiments. The approach provides insight into the functioning of the human at the information processing level.

The author further recommends that

- the micro-state model be expanded to include production rules and mental models of the tasks and situation. The model should also include training and motivation.

- higher cognitive functions be incorporated for multiple tasks involving crew interaction and communications, and navigation. The present study is limited to targeting tasks and does not consider the higher cognitive functions that are required of future combat vehicle operators. The study should include automated adaptive aiding for the performance of multiple tasks in future combat systems.

INTENTIONALLY LEFT BLANK

References

Allender, L. (April 1998). *Improved performance research integration tool (IMPRINT), user's guide (Version 4.0).* Aberdeen Proving Ground, MD: U.S. Army Research Laboratory.

Allender, L., Salvi, L., & Promisel, D. (April 1998). Evaluation of human performance under diverse conditions via modeling technology. In *Improved Performance Research Integration Tool (IMPRINT), User's Guide (Appendix A).* Aberdeen Proving Ground, MD: U.S. Army Research Laboratory.

Baltzley, D.R., Kennedy, R.S., Berbaum, K.S., Lilienthal, M.G., & Gower, D.W. (1989). The time course of post-flight simulator sickness symptoms. *Aviation, Space, and Environmental Medicine, 60(11)*, 1043-1048.

Brookhuis, K.A., DeVries, G., & De Waard, D. (1991). The effects of mobile telephoning on driving performance. *Accident Analysis and Prevention, 23(4)*, 309-316.

Card, S.K., Moran, T.P., & Newell, A. (1983). *The psychology of human-computer interaction.* Hillsdale, NJ: Lawrence Erlbaum Associates.

Charleton, S.G. (1996). Mental workload test and evaluation. *Handbook of Human Factors Testing and Evaluation*, T.G. O'Brien and S.G. Charlton (Eds.), Mahwah, NJ: Lawrence Erlbaum Associates.

Endsley, M.R. (1993a). A survey of situation awareness requirements in air-to-air combat fighters. *The International Journal of Aviation Psychology, 3(2)*, 157-168.

Endsley, M.R. (1993b). Situation awareness and workload: Flip sides of the same coin. In R.S. Jensen & D. Neumeister (Eds.), *Proceedings of the 7th International Symposium on Aviation Psychology* (pp.906-911), Columbus, OH: Department of Aviation, The Ohio State University.

Endsley, M.R. (1996). Situation awareness measurements in testing and evaluation. In *Handbook of Human Factors Testing and Evaluation*, T.G. O'Brien and S.G. Charlton (Eds.), Mahwah, NJ: Lawrence Erlbaum Associates.

Gordon, S.E. (1997). *An information-processing model of naturalistic decision making.* Presentation at Annual Meeting of the Idaho Psychological Association, Sun Valley, Idaho.

Hart, S.G., & Staveland, L. (1988). Development of the NASA Task Load Index (TLX): Results of empirical and theoretical research. In P.A. Hancock and N. Meshkati (Eds.) *Human Mental Workload,* pp. 139-183. Amsterdam: North-Holland.

Kennedy, R.S., Lane, N.E., Lilienthal, M.G., Berbaum, K.S., & Hettinger, L.J. (1992). Profile analysis of simulator sickness symptoms: Application to virtual environment systems. *Presence, 1(3),* 295-301.

Kennedy, R.S., Lilienthal, M.G., Berbaum, K.S., Baltzley, D.R. & McCauley, M.E. (1989). Simulator sickness in U.S. Navy flight simulators. *Aviation, Space, and Environmental Medicine, 60,* 10-16.

Kieras, D.E. (1988). Toward a practical GOMS model methodology for user se interface design. In M. Helander (ed.), *Handbook of Human-Computer Interaction* (pp. 135-157). Amsterdam: North-Holland.

Little, R., Dahl, S., Plott, B., Wickens, C., Powers, J., Tillman, B., Davilla, D., & Hutchins, C. (July 1993). *Crew reduction in armored vehicles ergonomic study (CRAVES)* (ARL-CR-80). Aberdeen Proving Ground, MD: U.S. Army Research Laboratory.

McCracken, J.H., & Aldrich, T.B. (1984). *Analysis of selected LHX mission functions: Implications for operator workload and system automation goals* (Technical Note ASI 479-024-84). Fort Rucker, AL: U.S. Army Research Institute Aviation Research and Development Activity.

Nelson, W.T., Hettinger, L.J., Cunningham, J.A., Brickman, B.J., Haas, M.W. & McKinley, R.L. (1998). Effects of localized auditory information on visual target detection performance using a helmet-mounted display. *Human Factors, 40(3),* 452-460.

Neter, J., Kutner, M.H., Nachtsheim, C.J., & Wasserman, W. (1996). *Applied linear statistical models,* New York: McGraw-Hill.

Norman, D.A. (1988). *The design of everyday things.* New York: Doubleday.

Pedhazur, E.J. (1982). *Multiple regression in behavior research: Explanation and prediction.* Chicago: Holt, Rinehart, and Winston, Inc.

Rasmussen, J. (1983). Skills, rules, knowledge: Signals, signs, and symbols and other distinctions in human performance models. *IEEE Transactions on Systems, Man, and Cybernetics, 13(3),* 257-267.

Rasmussen, J. (1986). *Information processing and human-machine interaction: An approach to cognitive engineering.* New York: Elsevier.

Rasmussen, J. (1993). Deciding and doing: Decision making in natural contexts. In G. Klein, J. Orasanu, R. Calderwood, and C.E. Zsambok (eds.), *Decision making in action: Models and methods* (pp. 158-171). Norwood, NJ: Ablex.

Selcon, S.J., Taylor, R.M., & Koritsas, E. (1991). Workload or SA?: TLX vs. SART for Aerospace systems design evaluation. *Proceedings of the Human Factors Society,* 35th Annual Meeting, 62-66.

Smyth, C.C. (1988). *A computer simulation model of outdoor radiant lighting* (Technical Note 10-80). Aberdeen Proving Ground, MD: U.S. Army Human Engineering Laboratory.

Smyth, C.C. (2002a). *Modeling indirect vision driving with fixed flat panel displays: Task performance and mental workload* (ARL-TR-2701). Aberdeen Proving Ground, MD: U.S. Army Research Laboratory.

Smyth, C.C. (2002b). *Detecting targets from a moving vehicle with a head-mounted display and sound localization.* (ARL-TR-2703). Aberdeen Proving Ground, MD: U.S. Army Research Laboratory.

Stein, E.S. (1993). Human operator workload. In M.W. Smolensky & E.S. Stein (Eds.), *Human Factors in Air Traffic Control* (p. 157). New York: Academic Press.

Taylor, R.M. (1988). Trust and awareness in human electronic crew teamwork. In T.J. Emerson, M. Reinecke, J.M. Reising, and R.M. Taylor (Eds.) The human–electronic crew: Can they work together? *Proceedings of a Joint GAF-USAF-RAF Workshop,* BSD-DR-G4. United Kingdom: RAF Institute of Aviation Medicine, Farnborough, Hants.

Taylor, R.M. (1989). SA rating technique (SART): The development of a tool for aircrew systems design. In *Proceedings of the AGARD AMP Symposium on SA in Aerospace Operations*, CP478, Seuilly-sur Seine: NATO AGARD.

Taylor, R.M., & Selcon, S.J. (1994). Situation in mind: Theory, applications, and measurement of SA. In R.D. Gilson, D.J. Garland, and J.M. Koonce (Eds.), *SA in Complex Systems*, Embry-Riddle Aeronautical University Press.

Warwick, W., McIlwaine, S., Hutton, R., & McDermott, P. (August 2001). Developing computational models of recognition-primed decision making. *Proceedings of the Driving Assessment 2001 Symposium*, 14-17.

Wickens, C.D. (1992). *Engineering psychology and human performance*. New York: Harper-Collins, Inc.

Wickens, C.D., Gordon, S.E., & Liu, Y. (1998). *Introduction to human factors engineering*. New York: Addison Wesley Longman, Inc.

Yardley, L. (1992). Motion sickness and perception: A reappraisal of the sensory conflict approach. *British Journal of Psychology, 83,* 449-471.

REPORT DOCUMENTATION PAGE

Form Approved
OMB No. 0704-0188

Public reporting burden for this collection of information is estimated to average 1 hour per response, including the time for reviewing instructions, searching existing data sources, gathering and maintaining the data needed, and completing and reviewing the collection of information. Send comments regarding this burden estimate or any other aspect of this collection of information, including suggestions for reducing this burden, to Washington Headquarters Services, Directorate for Information Operations and Reports, 1215 Jefferson Davis Highway, Suite 1204, Arlington, VA 22202-4302, and to the Office of Management and Budget, Paperwork Reduction Project (0704-0188), Washington, DC 20503.

1. AGENCY USE ONLY *(Leave blank)*	2. REPORT DATE June 2002	3. REPORT TYPE AND DATES COVERED Final

4. TITLE AND SUBTITLE

Modeling Workload for Target Detection From a Moving Vehicle With a Head-Mounted Display and Sound Localization

5. FUNDING NUMBERS

AMS Code 622716
PR: AH70

6. AUTHOR(S)

Smyth, C.C. (ARL)

7. PERFORMING ORGANIZATION NAME(S) AND ADDRESS(ES)

U.S. Army Research Laboratory
Human Research & Engineering Directorate
Aberdeen Proving Ground, MD 21005-5425

8. PERFORMING ORGANIZATION REPORT NUMBER

9. SPONSORING/MONITORING AGENCY NAME(S) AND ADDRESS(ES)

U.S. Army Research Laboratory
Human Research & Engineering Directorate
Aberdeen Proving Ground, MD 21005-5425

10. SPONSORING/MONITORING AGENCY REPORT NUMBER

ARL-TR-2759

11. SUPPLEMENTARY NOTES

12a. DISTRIBUTION/AVAILABILITY STATEMENT

Approved for public release; distribution is unlimited.

12b. DISTRIBUTION CODE

13. ABSTRACT *(Maximum 200 words)*

The effect of indirect vision systems on target detection and recognition is of interest to designers of future combat vehicles. In this report, a model of target detection and mental workload is described for an indirect vision system with a micro-state task time line analysis of attention workload. The model is based on the results of a field study in which participants detected and identified pop-up targets on an outdoor range from a stationary and a moving vehicle while using a head-mounted display (HMD), with and without sound localization and with direct viewing as a control. A head-slaved camera mounted on top of the vehicle provided the image to the HMD. As a result of the study, a target detection and identification model is derived for the different treatments from the data via regression analysis. The effect of indirect vision on mental workload is determined from the subjective ratings of perceived task loading that were reported in the field study. Along with the perceived workload, the study participants rated the mental measures of task-allocated attention, situational awareness, and motion sickness. Because of collinearity, the perceived workload is regressed on the factorial components of a cognitive loading space derived from a factorial analysis of the mental measures. Following rotation to a "skills-rules-knowledge" cognitive processing space derived from the clustering of the measures, the perceived workload is shown to be a function of the skill- and rule-based components. On this basis, a micro-state time line model is proposed for the task information processing. In addition to the attention allocated to the targeting task, the model includes attention to cognitive maps for target orienting by the audio cues and the monitoring of the internal somatic state for motion sickness. Further, the model includes switching between tasks (detection to identification) and the initial orienting and subsequent suppression responses to audio cues and body movements as intrusive stimuli. The task-loading measures generated by the model are compared to the reported values with significant results. Finally, the model results are used to construct information flow networks for task analysis workload simulation studies. The model is intended for future work in predicting fatigue and performance errors that are induced by mental workload during indirect vision targeting.

14. SUBJECT TERMS

modeling	situational awareness	workload
motion sickness	task allocation	

15. NUMBER OF PAGES
75

16. PRICE CODE

17. SECURITY CLASSIFICATION OF REPORT Unclassified	18. SECURITY CLASSIFICATION OF THIS PAGE Unclassified	19. SECURITY CLASSIFICATION OF ABSTRACT Unclassified	20. LIMITATION OF ABSTRACT

NSN 7540-01-280-5500

Standard Form 298 (Rev. 2-89)
Prescribed by ANSI Std. Z39-18
298-102